Sedimentary organic matter signature hints at the phytoplankton-driven Biological Carbon Pump in the Central Arabian Sea

Medhavi Pandey[1,2], Haimanti Biswas[1,2*], Daniel Birgel[3], Nicole Burdanowitz[3], Birgit Gaye[3]

[1]CSIR National Institute of Oceanography, Biological Oceanography Division, Dona Paula, Goa 403004. India.
[2]Academy of Scientific and Innovative Research (AcSIR), Ghaziabad-201002, India.
[3]Institute for Geology, Center for Earth System Research and Sustainability (CEN), Universität Hamburg, Bundesstraße55, 20146, Hamburg, Germany.
*Corresponding Author's email: haimanti.biswas.nio@gmail.com; haimanti.biswas@nio.org

Abstract

The Central Arabian Sea, a unique tropical basin is profoundly impacted by monsoon wind reversal affecting its surface circulation and biogeochemistry. Phytoplankton blooms associated with high biological productivity and particle flux occur in the northern part of the central Arabian Sea due to summer monsoon-induced open ocean upwelling and winter convection. The core Oxygen Minimum Zone (OMZ) at intermediate water depths is another important feature of the north-central Arabian Sea and fades southward. In this study, we attempt to interlink how these factors collectively impact phytodetrital export to the sediment. Short sediment core top (1 cm) samples representing the recent particle flux signatures were analyzed from 5 locations (21° to 11° N; 64° E) in the central Arabian Sea. Previously, we used core top (0-0.5 cm) samples and observed a trend between diatom frustule abundance and diversity with bulk sedimentary parameters indicating a spatial variability in phytodetrital export to the sediment. To verify this observation further, lipid biomarkers of key phytoplankton groups and a sea surface temperature (SST) proxy have been analyzed in addition to diatom frustules. The C_{37} alkenone-based SST proxy indicated cooler SST (27.6 ± 0.25 °C) in the north (21–15° N) mostly due to upwelling (summer) and convective mixing (winter). Warmer SSTs (+0.4 °C) are measured in the south, which usually remains nutrient-poor. This trend was consistent with satellite-derived average SST values (2017–2020). Lipid biomarker analysis suggests that dinoflagellates were likely to be the highest contributor as indicated by dinosterol and its degradative product dinostanol, followed by brassicasterol and C_{37} alkenone, likely representing diatoms and coccolithophores, respectively. The north, which largely experiences periodic phytoplankton blooms and is influenced by the thick OMZ, revealed the highest contents of organic matter, diatom frustules (diversity and abundance), dominated by large thickly silicified cells (e.g. *Coscinodiscus* and *Rhizosolenia*), and phytoplankton lipid biomarkers, as well as lower contents of zooplankton biomarkers (cholesterol and cholestanol). In contrast, relatively smaller chain-forming centric (e.g. *Thalassiosira*) and pennate (e.g. *Pseudo-nitzschia*, *Nitzschia, Thalassionema*) diatom frustules along with lower phytoplankton lipid biomarker contents were found in the south where zooplankton biomarkers and silicious radiolarians were more abundant. The possible impacts of OMZ on particle flux related to the phytoplankton community, including zooplankton grazing and other factors have been discussed.

Keywords: Phytodetritus; North Indian Ocean; Monsoon; Biomarkers; Brassicasterol; Dinosterol

1. Introduction

Marine phytoplankton modulate the global carbon cycle by fixing almost 48 Gt C annually (Singh and Ahluwalia, 2013) which corresponds to 50% of the global primary production (Field et al., 1998; Behrenfeld et al., 2006). This amount of organic matter produced within the euphotic layers, where more than 1% of sunlight arrives, supports the entire marine food chain including the benthic population. Nearly 10% of this organic matter (large and dense phytodetritus) sinks to the upper mesopelagic ocean and gets further fragmented by zooplankton and microbially remineralized on its descent into the deep ocean. Only 1–3% of this phytodetritus can reach the seafloor below 1000 m water depth (Iversen, 2023) and can be stored for hundreds to millions of years (Buesseler, 1998), and is called sequestration flux. This way of trapping carbon from the atmosphere to the ocean interior mediated by phytoplankton is called the Biological Carbon Pump (BCP) (Volk and Hoffert, 1985; Le Moigne, 2019; Iversen, 2023 and references therein). However, the organic matter in the surface sediment can be further modified biogeochemically. The strength of BCP is governed by many factors, such as heterotrophic remineralization of organic matter, dissolved oxygen (DO) levels, temperature, phytoplankton community composition, cell size, and zooplankton activity (Marsay et al., 2015; Keil et al., 2016; Cavan et al., 2017; Engel et al., 2017; Iversen, 2023). Out of multiple factors controlling the efficacy of the BCP, phytoplankton community composition (that controls organic matter stoichiometry), zooplankton grazing (Cavan et al., 2017), and mid-water oxygen concentrations (Keil et al., 2016) are crucial factors. Thus, understanding the functioning of the marine BCP in productive marine ecosystems needs attention, particularly in the context of changing climate (Iversen, 2023).

Diatom frustules, dinoflagellate cysts, and lipid biomarkers (e.g. sterols, alkenones) preserved in sediments could be potential proxies for the reconstruction of productivity and organic matter transport from the surface to the deep sea floor (Liu et al., 2013; Hu et al., 2020; Xiong et al., 2020 and references therein). The responses of phytoplankton to changing climate as well as other environmental variables can be retrieved from the sediments and may help predict future primary production, community shifts in marine ecosystems, and the ocean's role as a carbon sink. Generally, the siliceous frustules of diatoms are more resistant to grazing and degradation and can be better preserved in sediments compared to other phytoplankton groups. Sedimentary organic carbon, nitrogen, and their ratios, diatom frustules, and lipid biomarkers (e.g. sterols and alkenones) are used to reconstruct past phytoplankton community shifts and temperatures (Schubert et al., 1998; Liu et al., 2013; Rodríguez-Miret et al., 2023). The lipid biomarkers of phytodetritus from the surface sediments can also provide valuable information about the surface processes controlling phytoplankton growth (Xiong et al., 2020). For example in a study by Peng et al. (2023), phytoplankton community shift was evident from lipid biomarkers in the sediment core samples from the East China Sea. In a few studies, major phytoplankton-derived lipid biomarkers like dinosterol, brassicasterol, and alkenone were also used to correlate their contents with palaeoproductivity and associated changes of the sea ice levels in the Arctic Ocean (Müller et al., 2011, and references therein).

The Arabian Sea in the northwestern part of the Indian Ocean is a unique marine province with several characteristic features, for instance, the direct influence of monsoon winds on oceanographic and biogeochemical processes, high productivity (McCreary et al., 2009), and one of the thickest (200–1200 m) oxygen minimum zones (OMZ) in modern oceans (Banse et al., 2014). The entire area experiences periodic reversals of monsoon winds and surface circulation. During the summer (SW) monsoon, a low-level atmospheric jet (the Findlater Jet; Findlater, 1971) blows parallel to the Omani and Somalia coasts, generating coastal and open ocean upwelling in its northern part. Subsequently, due to natural nutrient enrichment, phytoplankton blooms develop (Banse, 1987; Bhattathiri et al., 1996; Prasanna Kumar et al.,

2000). In the winter (NE) monsoon, winds and surface circulation reverse and in the northern Arabian Sea, the cooling and densification of surface water leads to convective mixing (Prasannakumar et al., 2001) that also fuels high phytoplankton growth (Madhupratap et al., 1996).

In the Arabian Sea, the magnitude of particle transfer to the deep sea floor is directly controlled by the surface processes (Schulte et al., 1999, Rixen et al., 2019a). The central Arabian Sea exhibits one of the highest particle flux rates (1.3–3.3 g C m^{-2} $year^{-1}$) (Haake et al., 1993) compared with other low-latitude seas (Rixen et al., 2019b). This is mostly associated with enhanced biological productivity governed by summer monsoon-induced upwelling and winter convection (Nair et al., 1989; Haake et al., 1993; Rixen et al., 2019a). Nevertheless, particle flux could vary significantly (Nair et al., 1989; Prahl et al., 2000) during the intermonsoon and premonsoon due to prevailing oligotrophy (Prasanna Kumar and Narvekar, 2005).

The impacts of atmospheric forcings and consequent biological response in the central Arabian Sea have been studied thoroughly during the joint Global Ocean Flux Studies (JGOFS, from 1987 to 2003). The monsoon wind is the major controlling forcing of physical, chemical, and biological processes in the surface ocean (McCeary et al., 2009) with high spatial and seasonal variability (Prasanna Kumar and Narvekar, 2005). However, there has been no further investigation in the last two decades, although ocean warming continued with high spatial variability (Roxy et al., 2016; Sharma et al., 2023 and references therein). Our previous study showed that diatom frustules retrieved from the surface sediments from the central (Pandey et al., 2023) and the eastern (Pandey and Biswas, 2023) Arabian Sea could be an efficient indicator of surface processes controlling euphotic phytoplankton communities. There are a few studies from the Arabian Sea characterizing sedimentary organic carbon using phytoplankton biomarkers (Schubert et al., 1998; Prahl et al., 2000; Schulte et al., 1999; 2000) suggesting such proxies from the surface sediment may be quite useful to understand the spatial variability in organic matter transport. Prahl et al. (2000) used phytoplankton biomarkers (e.g. C_{37}-alkenones, dinosterol, β-sitosterol) from sediment trap samples as well as from the surface sediments over a year from the central Arabian Sea (15°59′N, 61°30′E) and showed the seasonal variability of biological productivity. Nevertheless, the degradation of organic matter in the water column could be quite high during their descent through the water column pointed out by Wakeham et al. (2002) in their work on lipids from the water column of the western Arabian Sea.

Importantly, the Arabian Sea is warming at a faster pace compared to other oceanic regions (Roxy et al., 2016; Sharma et al., 2023), and how the phytoplankton-driven organic matter transport may respond to that change is still poorly understood. Furthermore, recent modeling studies (Vallivattathillam et al., 2023) as well as data from biogeochemical-Argo floats (Liu et al. 2024) hinted at a possible thinning of the OMZ in the Arabian Sea that may substantially impact organic matter degradation within the water column, specifically in the southern part (Roxy et al., 2016). To fill this gap, we want to address three major questions in this study, 1) Which phytoplankton group dominates the sedimentary organic matter in the various stations of the transect from north to south? 2) Does high spatial variability in the phytoplankton community composition driven by physical forcing also impact organic matter transport? 3) What are the possible factors (hydrography, physicochemical conditions, and atmospheric forcings) being responsible for such spatial variability in organic matter transport in this region? To address these questions, we have measured key parameters from surface sediments including lipid biomarkers, alkenone-based SST reconstruction, and diatom frustules combined with a few recent in-situ observations on hydrography, biogeochemistry, and phytoplankton

community from the central Arabian Sea (Silori et al., 2021; Chowdhury et al., 2021; Pandey et al., 2023; Chowdhury et al., 2024). In our previous study (Pandey et al., 2023) using the core top (0–0.5 cm) samples we observed a trend between diatom frustules abundance and diversity with sedimentary parameters and atmospheric forcings. In this study, lipid biomarkers of other phytoplankton groups including diatoms are considered to understand their contribution to organic matter flux. Further, a lipid biomarker as an SST proxy has also been studied to correlate with atmospheric forcings.

2. Methodology

2.1. Sample collection

During cruise SSD–068 (Dec 2019 to Jan 2020) with *RV. Sindhu Sadhana* five short sediment cores were obtained using a multicorer (Ocean Scientific International Limited Maxi Multi-corer; core tubes 60 cm, outer diameter 11 cm and 10 cm inner diameter) along a transect from 11–21° N at 64° E (Fig. 1a). These short cores were collected at 21° N, 19° N, 15° N, 13° N, and 11° N with varying water depths between 3000 m and 4500 m (Fig. 1a). The cores were subsampled onboard immediately in 0.5 cm slices and were kept in pre-cleaned plastic containers at 0–4 °C. The advantage of using a multicorer is better preservation of the topmost parts of the sediment core compared to other devices like box or gravity coring (Barnett et al., 1984). For this study, we used the top 1 cm (0–0.5 cm and 0.5–1 cm slices) of cores for all related analyses. Note that the core top samples (0–0.5 cm) were analyzed for total inorganic carbon (TIC), total organic carbon (TOC), total nitrogen (TN) as well as diatom frustules and diversity including radiolarian abundance earlier by Pandey et al. (2023).

2.2. Analytical method

2.2.1. Total inorganic carbon (TIC), total organic carbon (TOC), and total nitrogen (TN) contents

Sediment samples (0.5–1 cm) were dried at 60 °C overnight and ground using agate mortar and pestle. Aliquots (10 mg) of sediment samples were taken in tin capsules. Total carbon (TC) and TN were measured using a CHN Elemental analyzer (Euro Vector EA3000 series analyzer) at the Central Analytical Facility of CSIR-National Institute of Oceanography, Goa, India) against soil reference material NC soil standard (5g 338 40025 procured from Elemental Microanalysis Ltd, UK, Soil Standard Clay OAS Cat No. B2051–Certificate No. 341506) used for carbon and nitrogen with an analytical error of < 2%. The TIC contents were measured against the calcium carbonate ($CaCO_3$) standard (Merck, Germany) in a coulometer attached to an acidification module (Model CM5015 (UIC, USA). The accuracy and precision obtained from the results were within ± 1.25%. TOC values were calculated by the difference between TC and TIC (TOC =TC-TIC).

2.2.2. Analysis of silica-bearing organisms from sediments

The diatom frustules and other siliceous organisms from sediments (0.5–1 cm) were enumerated following the method by Armbrecht et al. (2018). The dried sediment subsamples (50 mg) were taken in a 15 mL sterile polypropylene tube and were treated chemically with 10% HCl, 30% H_2O_2, and 0.01 N anhydrous sodium diphosphate ($Na_4P_2O_7$) for removing carbonate, organic matter, and fine clay, respectively. After each chemical treatment, samples were washed three times with 15 mL Milli-Q water. Finally, the residue remaining after the last rinse and decantation was diluted with Milli-Q to 10 mL and was homogenized. A small portion (1 mL) from this homogenized solution was analyzed under an inverted microscope

(Nikon Ti2) in a Sedgewick rafter counting chamber (Pyser, UK) at 400–600× magnification. The classical identification keys by Tomas (1997), Desikachary (1989), and http://www.algaebase.org were used. No centrifugation was used in this process to avoid the breaking of frustules. Further, the diatoms more than half in size were considered complete valves (Abrantes and Sancetta, 1985). The diatom abundance was expressed as valves g^{-1} dry sediment. Radiolarians were also enumerated along with diatom frustules and given as individuals g^{-1}.

2.2.3 Biomarker analysis and SST proxy

Lipid biomarker analyses were carried out at the Institute for Geology, University of Hamburg, Germany. About 11 g to 19 g of freeze-dried and ground samples were used to obtain total lipid extracts (TLEs) by using an Accelerated Solvent Extractor (ASE200, DIONEX). Before extraction, a known amount (10 ng μL^{-1}) of internal standards (14-heptacosanone, nonadecanol, and dialkylglycerol ether-18 (DAGE-18)) were added to the samples. The ASE extraction for each sample was carried out at 100°C and 1000 PSI for 5 minutes in 3 cycles by using the solvent mixture dichloromethane: methanol (DCM: MeOH, 9:1). The TLEs were then concentrated with rotary evaporation and were separated later into a hexane-soluble (adding *n*-hexane) and hexane-insoluble (adding DCM) fraction via $NaSO_4$ column chromatography. To separate the hexane-soluble fraction into a neutral- and acid fraction via saponification (at 85°C for 2 hrs) a 5 % potassium hydroxide (KOH) in MeOH solution was added to this fraction. Then, the neutral fractions were obtained by adding n-hexane to the saponified fraction, vortexing, and pipetting the neutral fraction containing *n*-hexane layer into a new vial. The neutral fractions were then separated into apolar-, ketone- (containing alkenones), and polar fractions (containing sterols, stanols) by column chromatography packed with deactivated silica gel (5 % H_2O, 60 µm mesh) using the solvents n-hexane, DCM, and DCM: MeOH (1:1), respectively. We took 50% splits of the ketone- and polar fractions and put them together, as some of the sterols and added standards for the sterol fraction were found in the ketone fraction, too. For the derivatization of these fractions, a mixture of 200 µL BSTFA: Pyridin (1:1) was added to the dried sample and heated at 80°C for 2 hrs followed by drying under an N_2 environment.

To quantify the alkenones and sterols the samples were measured with a Thermo Scientific Trace 1310 gas chromatography coupled to a flame ionization detector (GC-FID) equipped with a Thermo Scientific TG-5MS column (30 m, 0.25 mm, 0.25 µm). H_2 as carrier gas was used with a flow rate of 35 mL $minute^{-1}$ and the PTV injector started at 50°C ramped with 10°C/s to 325°C in a splitless mode. For the alkenones, the initial GC temperature was programmed to 50°C (held 1 minute) and then ramped to a temperature of 230 °C with an increased rate of 20 °C $minute^{-1}$, then increased at 4.5°C $minute^{-1}$ to 260 °C, and at 6 °C $minute^{-1}$ to 325 °C, which was held for 15 minutes. The peaks of alkenones were identified by comparing the retention time for peaks of the samples with a known working sediment standard. Quantification of the alkenones was done by using 14-heptacosane and tetratriacontane with a known amount (10 ng μL^{-1}) as external standards. Repeated measurements of the external standards yielded a quantification precision of 13 % (14-heptacosanone) and 8 % (tetratriacontane). The alkenone saturation index was calculated using the equation by Prahl et al. (1988):

$$U_{37}^{k\prime} = \frac{C_{37:2}}{C_{37:2} + C_{37:3}}$$

to convert the $U_{37}^{k\prime}$ index to SSTs we have used the core top calibration of Indian Ocean sediments (Sonzogni et al., 1997):

$$SST = \frac{U_{37}^{k\prime} - 0.043}{0.033}$$

For each sample, at least a duplicate measurement was conducted, which yielded an average precision of 0.1°C (1SD). Replicate extractions of a working standard sediment (n=2) and its duplicate measurements where each replicate yielded an average precision of 0.5°C (1 SD).

For the quantification of the sterols, the initial GC temperature was 50°C (held for 3 minutes) and then programmed to a final temperature of 325 °C (held for 20 minutes) with an increase of 6 °C minute^{-1}. To quantify the sterols we used nonadecanol and DAGE-18 with a known amount (10 ng µL) as external standards, with precision of 5.6 % and 4.9 %, respectively. To identify the sterols the mass spectra of each sample were investigated using a Thermo Scientific Trace GC Ultra coupled to a Thermo Scientific DSQ II mass spectrometer (GC-MS). He (2 mL minute^{-1} flow rate) was used as carrier gas. The initial GC temperature was 50 °C (held for 3 minutes) and ramped with 6 °C minute^{-1} to 325 °C (held for 25 minutes). The mass spectra of the compounds were then compared with published mass spectral data.

2.2.4 Sea surface temperature (SST) and Chlorophyll *a* (Chl*a*) from satellite imagery

The SST data was accessed from the climate reanalysis version 5 (ERA5) of the European Centre for Medium-Range Weather Forecasts (ECMWF) (C3S, 2017). ERA5 covers the time from 1979 to the present at a 0.25° × 0.25° grid. In this study, we used monthly mean of SST data averaged for a period from 2017–2020 (downloaded from https://cds.climate.copernicus.eu/cdsapp#!/dataset/reanalysis-era5-single-levels?tab=form. Chl*a* values were derived from Aqua MODIS at a 4 km resolution. The average was calculated from daily Chl*a* data during the period of 2017 Jan to 2020 Dec (downloaded from https://oceancolor.gsfc.nasa.gov/l3/).

2.2.5 Statistical analysis

The Shapiro-Wilk normality test and F test were used to check the normality and variance of individual datasets, respectively. The statistical significance between differences for various parameters was obtained using single-factor Analysis of Variance (ANOVA) in Microsoft Excel 2019 at a 95% confidence level (probability $p<0.05$). The correlations between the biotic and environmental variables were derived using a linear multivariate model RDA (Redundancy Analysis). The relationships between the key variables (biomarkers, frustules, radiolarian, diatom community, TOC, TN, TOC: TN, TIC, and SST) are tested using the CANOCO version 4.5 software (Ter Braak and Šmilauer, 2002). In this test, cluster I contained biomarkers, frustules, radiolarian, and diatom community, and cluster II included other variables (SST, TOC, TN, TIC, TOC: TN).

3. Results

The sedimentary characteristics (TIC, TOC, TN), diatom frustule abundance, and diversity including radiolarian abundance from this study (0.5–1 cm depth) and by Pandey et al. (2023, core top 0–0.5 cm) are shown as average representing the top 1 cm of the surface sediment (Table 1). Results of lipid biomarkers (0–0.5 and 0.5–1 cm) such as various phytosterols and the summed $C_{37:2}$ and $C_{37:3}$ alkenones as well as $U_{37}^{k\prime}$-derived sea surface temperatures (SSTs) are shown in Table 1. For further discussion of our results, the study area has been defined as a northern part (north of the mean position of Findlater Jet) including sites 21 ºN, 19 ºN, and 15º N; and a southern part including sites 11 ºN, and 13 ºN (Fig. 1a).

3.1 Bulk sedimentary analysis and SST reconstruction

To compare with $U_{37}^{k'}$ based-SST reconstruction, we present the SST values derived from satellite data (Fig. 1b) averaged for the years 2017–2020. High spatial variability in SST is observed from the north (mean 27.4°C) to the south (28°C). The surface chlorophyll*a* (Chl*a*) value average from 2017-2020 is shown in Fig. 1c. A distinct north-south variability is noticed with higher Chl*a* values (~1–2 mg m^{-3}) in the north and lower values in the south (~0–0.5 mg m^{-3}). TIC contents (Fig. 2a) are slightly higher in the south (7.06 ± 0.63 %) compared to the north (5.15 ± 1.57 %) and this difference is statistically significant at a 94.7 % confidence level (single factor ANOVA analysis, Table 2). TOC contents (Fig. 2b) are substantially higher (p <0.001) above 15° N (0.97 ± 0.06 %) reaching their highest value at 21° N and decreased southward (0.78 ± 0.005 %). TN values (Fig. 2c) revealed a similar trend as TOC and decreased from 21° N (0.11 ± 0.001 %) to 11° N (0.07 ± 0.009 %). The average TN value (0.06 ± 0.008 %) in the south is significantly lower (p <0.001) compared to the north (0.087 ± 0.018 %). The ratio of TOC and TN (Table 1) is the lowest (9.5 ± 0.18) in the north at 21° N and increased at the rest of the stations reaching >12. The $U_{37}^{k'}$ based SST (Fig. 2d) shows an average value of 27.8 ± 0.3 °C. The coolest reconstructed SSTs (27.6 ± 0.25 °C) are found in the north and are nearly 0.4 °C cooler compared to the south (p <0.05) (Table 2).

3.2 Lipid biomarkers

The lipid biomarkers brassicasterol (Fig. 2e), dinosterol (Fig. 2f), dinostanol, the saturated, degradative product of dinosterol (Fig. 2g), summed $C_{37:2 \text{ and } 37:3}$ alkenones (C_{37} alkenone) (Fig. 2h), cholesterol (Fig. 2i), and its degradative product cholestanol (Fig. 2j) are present in the surface sediments from north to south.

Among phytoplankton lipid biomarkers, the average dinosterol contents (98 ± 64 ng g^{-1}) found in the surface sediment are the highest followed by brassicasterol (64 ± 44 ng g^{-1}) and then C_{37} alkenones (39.4 ± 12 ng g^{-1}) (Table 1) and show significant linear positive correlations (R^2 =0.62–0.96, p< 0.05) with each other. All three biomarkers show the highest concentrations at the northernmost station at 21° N (Fig. 2; Table 1) and decrease to their minimum values at 11° N. The sum of the major biomarkers (brassicasterol, dinosterol, and alkenones) representing the major three phytoplankton groups, with the highest concentrations (33.9 ± 14.13 µg g^{-1} TOC) occur at 21° N compared to other stations (19.96 ± 9.5 µg g^{-1} TOC) (Fig. 2). The TOC normalized values of dinosterol (16.53 ± 8.3 µg g^{-1} TOC) and brassicasterol (12.37 ± 5.2 µg g^{-1} TOC) are the highest at the northernmost station and decrease southward. However, the average values of dinosterol (north: 12.81 ± 6.3 µg g^{-1} TOC; south 7.8 ± 4.47 µg g^{-1} TOC) and brassicasterol (north: 8.64 ± 4.75 µg g^{-1} TOC; south 5.81 ± 3.48 µg g^{-1} TOC) are not significantly different (p>0.05) (Table 2). The average ratios of dinosterol to brassicasterol and brassicasterol to alkenones are 1.5 and 1.6 (Table 1), respectively, without any significant north-south variability (Table 2). However, none of the biomarkers showed any statistically significant difference in their TOC normalized values between the stations.

Cholesterol (Fig. 2i), mostly varied between 10 ± 2.5 µg g^{-1} TOC (north) and 14.3 ± 5.8 µg g^{-1} TOC (south) without any statistical significance. The TOC normalized values of cholestanol (Fig. 2j) are lower in the northern (11.8 ± 6.3 µg g^{-1} TOC) than in the southern part (15.9 ± 11.4 µg g^{-1} TOC) and no significant correlation was noticed (Table 2).

3.3 Silicious organisms: Radiolarians and diatoms

Radiolarian abundance (Fig. 2k) in the central Arabian Sea varied between 1.07 and 2.13 × 10^4 individuals g^{-1} with the highest numbers at 13° N and the lowest at 21° N. Their occurrences are found to be higher at the southern stations (1.84 × 10^4 individuals g^{-1}) compared to northern stations (1.10 × 10^4 individuals g^{-1}) with statistical significance (p<0.05) (Table 2). The

community is dominated by the genus *Tetrapyle* sp. and their abundance was higher in the south.

Diatom frustules from the surface sediments show high spatial variability in both abundance and diversity. The total frustule abundance in the central Arabian Sea (Supplementary Table 1; Fig. 2l) ranges between 2.78 and 6.36 × 10^4 valves g^{-1}. The highest frustule abundance is observed at 19–21° N and the least at 11° N. At station 19° N, the frustule abundance is the highest (6.36 ± 0.2 × 10^4 valves g^{-1}) among all stations (Table 1). The frustule numbers found in the north (5.46 ± 0.95 × 10^4 valves g^{-1}) are 1.67 times higher than in the south (p<0.01). Diatom frustule diversity has been calculated to understand the north-south distribution pattern and the average Shannon–Wiener diversity index (H′) is 1.6 ± 0.1 with the highest diversity at 21° N (1.8) (Supplementary Fig. 1). Microscopic analysis reveals a total of 23 genera, with 9 centric and 14 pennate diatoms. More than five-fold higher abundance of centric diatoms is observed than pennate at all the locations (p<0.05).

The overall diatom community in the sediment samples from the central Arabian Sea (Supplementary Table 1; Fig. 3) is observed to be dominated by *Coscinodiscus* (40%), *Thalassiosira* (34%), *Pseudo-nitzschia* (6%), *Rhizosolenia* (4%), *Hemidiscus* (4%), *Thalassionema* (4%), and *Nitzschia* (3%). The northern stations are dominated by *Coscinodiscus* sp., whereas the two southernmost stations are dominated by *Thalassiosira* sp. In the north, the highest abundance (2.46 × 10^4 valves g^{-1}) of *Coscinodiscus* sp. was observed (p<0.05) with the least abundance at 11° N (0.61 × 10^4 valves g^{-1}). In the south, *Thalassiosira* seemed to dominate (1.59 × 10^4 valves g^{-1}) without any statistical significance. The Bray-Curtis similarity index usually indicates the similarity in the distribution pattern of different diatom genera/species. The results reveal (Supplementary Fig. 2) that the two dominating diatom genera, i.e. *Coscinodiscus* sp. and *Thalassiosira* sp. are grouped showing a similar distribution pattern. The commonly occurring pennate diatom *Pseudo-nitzschia* is present independently, whereas, *Rhizosolenia* and *Thalassionema* are grouped. The other two major contributing diatom genera, *Hemidiscus* and *Nitzschia* reveal a similar pattern.

3.4 Statistical analyses

In the RDA biplot (Fig. 4), Axis 1 and 2 explained most of the variability (~97.2%). The biotic variables and all other environmental parameters show a distinct association. Interestingly, TOC, TN, the key phytoplankton biomarkers (dinosterol, brassicasterol, dinostanol, and alkenones), along with diatom frustules abundance, and the major genera are grouped and are at the opposite axis where TIC, SST, cholesterol, and radiolarian were together. The association between the larger diatoms like *Coscinodiscus* and *Rhizosolenia* and organic matter including brassicasterol depicts that the organic matter flux is coupled with diatom fluxes. The positioning of *Thalassiosira* opposite these parameters also suggests that its abundance is higher in the south associated with warmer SSTs. TOC: TN ratio and TIC along with SST are found to be closely related in the RDA plot (Fig. 4).

4. Discussion

4.1 Physical forcing induced spatial variability in physicochemical properties

The alkenone-derived SST suggests a cooler northern part compared to the south along the sampling transect (64° E, Fig. 2d). The annual average of satellite-derived SST also revealed a similar trend. Such variability in SST from north to south could be attributed to monsoon wind variability and related processes. During the summer monsoon, the physicochemical parameters (wind speed, SST, nutrients, mixed layer depths [MLDs]) along 64° E show distinct north-south demarcation due to the presence of the Findlater Jet (Findlater, 1971). In the northern flank of this jet axis, the maximum influence of upwelling is evidenced by the

presence of cooler SSTs, high nutrient levels, and shallower MLDs (Silori et al., 2021; Chowdhury et al., 2021; Chowdhury et al., 2024). Along the axis (~15–18° N) of the Jet the highest wind speeds are recorded (Silori et al., 2021; Chowdhury et al., 2021; Chowdhury et al., 2024). The coolest SST value at 15° N is most likely due to the advection of cool nutrient-rich upwelled waters from the western coastal Arabian Sea (Bauer et al., 1991). Furthermore, such high wind speeds for a prolonged period may also lead to evaporative heat loss leading to a decrease in SST. Contrarily, in the south downwelling induced deeper MLDs (>100 m), nutrient-poor waters along with higher SSTs are observed (Latasa and Bidigare, 1998; Chowdhury et al., 2021; Silori et al., 2021). During the winter monsoon, surface circulation reverses in this region, and in the northern Arabian Sea cold dry wind leads to evaporative cooling and subsequent convection leading to cooler SSTs, and high nutrient levels. At the same time, southern regions remain oligotrophic and warm. During the intermonsoon and premonsoon, SST increases and nutrient level reduces substantially along the entire transect (Prasannakumar and Narvekar, 2005). Consistent with this fact, the annual average satellite-derived Chl*a* values (Fig. 1c) also indicated higher phytoplankton biomass in the north induced by nutrient enrichment, whereas the south was mostly low productive.

4.2 Spatial variability in particle flux, and phytoplankton dynamics

4.2.1 Organic matter

The northernmost stations were the hotspots for particulate organic matter (POM) flux and sink to the sediment floor (Fig. 2). The positioning of SST in the RDA plot (Fig. 4) opposite TOC, TN, diatom frustules, and phytoplankton lipid biomarkers also supported this fact. The north-south variability in phytodetritus flux could be also influenced by dissolved oxygen levels within the mesopelagic zone (Fig. 5) as it directly controls microbial degradation and zooplankton activity (Moriceau et al., 2018; Iversen, 2023). In our sampling transect, the northern stations are under the influence of intense oxygen deficiency which decreases in intensity and thickness towards the south (Banse et al., 2014). In their synthesis, Banse et al. (2014) showed that the median DO values within 150–500 m depth in the northern stations within the core OMZ vary between 0.04 and 0.30 mL L^{-1}. Conversely, in the south, these values increased to 0.24–0.72 mL L^{-1}. Such spatial variability in OMZ distribution/intensity across the stations could substantially alter the rate of organic matter mineralization, zooplankton abundance (Cavan et al., 2017), and particle flux attenuation (François et al., 2002; Keil et al., 2016). Fast and efficient mineralization within the mesopelagic may allow less organic matter to be transported, whereas partial remineralization may lead to higher organic matter export flux (Ragueneau et al., 2006). Therefore, the northern stations at an intense OMZ may have a higher preservation potential of organic matter compared to the south (Fig. 5) as mentioned by Schulte et al. (2000).

4.2.2 Lipid biomarkers as indicators of phytoplankton and zooplankton

Phytoplankton and zooplankton produce specific lipid biomarkers that are stored in ocean sediments (Castañeda and Schouten, 2011; Meyer 1997; Volkman et al., 1998; Volkman, 2003) and are commonly used to reconstruct past environmental changes (Castañeda and Schouten, 2011; Eglinton and Eglinton, 2008). For instance, calcifying nanophytoplankton *Gephyrocapsa huxleyi* (also known as *Emiliania huxleyi*) and *Gephyrocapsa oceanica* are known to be the main producers of C_{37} ($C_{37:2}$ and $C_{37:3}$) alkenones in the ocean (Brassell et al., 1986; Eglinton and Eglinton, 2008; Prahl and Wakeham, 1987). In modern and past climate studies $C_{37:2}$ and $C_{37:3}$ alkenones are used extensively as reliable SST proxies (Prahl et al., 1988; Sonzogni et al., 1997). Among sterols, dinosterol and its degradative product dinostanol are often used as a proxy to represent dinoflagellates (Meyers, 1997; Castañeda and Schouten, 2011).

Brassicasterol a commonly used biomarker of diatoms, may be produced by other microalgae (Volkman et al., 1998). For example, haptophytes and dinoflagellates produce minor contents of brassicasterol, depending on physicochemical parameters like nutrient availability and temperature (Ding et al., 2019). Brassicasterol contents could be higher in diatoms under a balanced N:P supply, whereas a reduced N:P leads to higher brassicasterol production in dinoflagellates (Ding et al., 2019). Nevertheless, brassicasterol is produced by most of the pennate diatoms as major sterol, however, the quantity may vary substantially in radial centric diatoms (Véron et al., 1998). Although we do not have enough experimental/field evidence to disapprove that brassicasterol is produced solely by diatoms and hence could be a valid proxy for this group, several studies show that many diatoms produce brassicasterol in significant amounts, specifically pennates and also many radial centric diatoms (Véron et al. 1998; Ding et al., 2019; Jaramillo-Madrid, et al., 2019; Jaramillo-Madrid, et al., 2020). Likewise, we are using brassicasterol to indicate the presence of diatoms as a group in the sedimentary organic matter without assigning this lipid biomarker to any specific phylogenetic group, genera, or species to indicate the sources.

TOC-normalized lipid biomarker contents indicate the relative contribution of major phytoplankton groups to total organic matter found in surface sediments. Both total and TOC-normalized phytoplankton lipid biomarkers revealed that dinoflagellates, diatoms, and coccolithophores were the dominant phytoplankton groups (Fig. 2). All studies available from the Arabian Sea using biomarkers (Schubert et al., 1998; Schulte et al., 1999; 2000; Prahl et al., 2000) showed that dinosterol contents were higher than brassicasterol, both in sediment core and trap samples, suggesting greater contributions of dinoflagellates compared to diatoms. Likewise, we also observed nearly 1.5 times higher dinosterol contents compared to brassicasterol. The dominance of dinosterol, C_{37}-alkenones, and some species-specific lipid biomarkers for diatoms was found in sediment trap samples (2220 m depth) from the central (Prahl et al., 2000), in two sediment core samples from the northeastern and southern Arabian Sea (Schulte et al., 1999). Further, a long sediment core from the northern Arabian Sea close to our sampling locations (22° 29.31′ N, 65° 38.9′ E) (Schubert et al., 1998) also reported the same dominating phytoplankton groups in the Arabian Sea over the past 0.2 million years.

Since diatoms predominate over dinoflagellates during phytoplankton blooms (Chowdhury et al., 2021; 2024) a higher contribution of brassicasterol over dinosterol should be expected, however, it was the opposite in our study. This reverse trend can be explained by the seasonal succession of phytoplankton communities in surface layers mostly driven by nutrient stoichiometry related to monsoon wind forcings and grazing (Prahl et al., 2000; Rixen et al., 2019a). It should be noted that organic matter on the surface sediment accumulates throughout the year with variable depositional rates. Monsoon reversal also leads to changes in the phytoplankton community (Sawant and Madhupratap, 1996; Latasa and Bidigare, 1998) that may also affect the transfer of phytodetritus to the sea floor. Consequently, diatom frustules largely represent the signature of the most productive seasons. In contrast, the nutrient-poor phases are usually dominated by dinoflagellates and other calcifying nanophytoplankton. Dinoflagellates grow slowly in nutrient-poor warm waters and can remain there for longer periods (k-strategists) (Smayda and Reynolds, 2001; Glibert et al., 2016). Likewise, this situation can be found at the southern stations, where high SSTs and oligotrophic conditions were more favorable for the growth of dinoflagellates (Chowdhury et al., 2021; 2024). This is reflected south of the 15° N station by the occurrences of dinoflagellates like *Gymnodinium* sp., *Gyrodinium* sp, and *Katodinium* sp. with small cells (Garrison et al., 1998; Chowdhury et al., 2021).

Moreover, unlike diatoms, which are photoautotrophs, most dinoflagellates could be either heterotrophs or mixotrophs (Stoecker, 1999; Stoecker et al., 2017) which actively graze on smaller phytoplankton including diatoms and even could be detritivorous feeding on particles (García-Oliva et al., 2022). Mixotrophs could consume prey to meet their cellular nitrogen demand and can simultaneously perform photosynthesis to gain carbon (Stoecker et al., 2017). In the Arabian Sea, a significant part of the dissolved inorganic nitrogen is lost due to strong denitrification within the OMZ and often becomes the growth-limiting nutrient for phytoplankton (Ward et al., 2009). Therefore, particularly during the stratified oligotrophic phases like intermonsoon and premonsoon, when SST increases fostering stratification, nanophytoplankton, and dinoflagellates dominate over diatoms. Hence, the overall contribution of dinoflagellates on an annual basis could exceed diatoms as dinoflagellates are constantly present during both high-nutrient regimes and low-nutrient stratified warm water periods.

Another possible factor for the observed variability in brassicasterol to dinosterol could be due to differences in their labile nature. It was claimed that diatom-rich organic matter could be of higher lability (François et al., 2002) and may possess low transfer potential to the sea floor (Alonso-González et al., 2010). Contrary to this, it was also observed that compared to other phytoplankton (Cabrera-Brufau et al., 2021) diatom-rich organic matter is more of a refractory nature against mesopelagic microbial degradation. Moreover, the phytodetritus of diatom origin could be preferably consumed by the benthic communities than other phytoplankton groups (Nomaki et al., 2021) and could be one of the reasons for lower brassicasterol over dinosterol in the surface sediment. This is indeed difficult to conclude as we do not have enough experimental evidence supporting/contradicting these hypotheses. Further, as mentioned before we can not exclude, that brassicasterol is sourced by other phytoplankton groups than diatoms.

In the central Arabian Sea, coccolithophores constitute an important part of the nanophytoplankton community (Andruleit et al., 2004; Schiebel et al., 2004; Mergulhao et al., 2006). The relatively high occurrences of substantial amounts of C_{37}-alkenones all along the transect in our study indicate that coccolithophores may also contribute as a major part of sinking phytodetritus, with slightly higher values towards the north (Fig. 2h). Sediment trap studies from the south of the Findlater Jet (Mergulhao et al., 2006) reported the flux of coccolithophores throughout the year justifying our observations.

4.2.3 Diatom frustules

In our previous study (Pandey et al., 2023), using the topmost (0–0.5 cm) part of the cores, a trend in diatom frustule abundance and diversity from north to south was observed. After compiling the data from 0.5 to 1 cm a similar trend was noticed. The highest abundance of diatom frustules coupled with TOC and TN contents was found in the northern stations, which most likely indicated higher organic matter transfer to the sediment compared to the southern stations. The RDA plot (Fig. 4) also revealed that the abundance of large centric diatoms like *Coscinodiscus, Rhizosolenia,* TOC, and TN contents as well as brassicasterol were grouped and correlated significantly. In this context, it should be noted that the correlation between brassicasterol and the major diatom taxa does not necessarily suggest that they are the sole producers of this lipid biomarker as mentioned in the previous sections. This correlation most probably indicates that the highest production of brassicasterol and diatom bloom might have cooccurred and during this period, large diatoms like *Rhizosolenia* or *Coscinodiscus* also dominated with many other centric and pennate diatoms that produce brassicasterol.

During both summer (Chowdhury et al., 2021) and winter monsoons (Sawant and Madhupratap, 1996) in the northern Arabian Sea, *Coscinodiscus* and *Rhizosolenia* are the

major diatoms forming blooms and consequently, dominate the flux of biogenic silica (Rixen et al., 2019a). A higher abundance of large *Rhizosolenia* frustules was also seen in the sediment trap samples from the central Arabian Sea after the summer monsoon bloom (Rixen et al., 2019a). The contribution of heavily silicified diatom frustules may in addition provide ballasting effects (Smetacek, 1985; Tréguer et al., 2018) facilitating efficient organic matter export compared to other phytoplankton groups (Buesseler, 1998; Boyd and Newton, 1999; Zúñiga et al., 2021). Diatom bloom development in the Arabian Sea was found to be associated with dissolved silica (DSi) availability (Chowdhury et al., 2021) and the depth of the silicicline (Anju et al., 2020). The northern stations become DSi depleted (<2 μM) at the end of the bloom (Chowdhury et al., 2021) and may lead to a mass sinking of frustules (Smetacek, 1985; Krause et al., 2019) or they can be grazed and cell death may also occur due to viral attacks (Agusti and Duarte, 2000). On the other hand, the abundance of small chain-forming diatoms such as *Thalassiosira*, *Pseudo-nitzschia*, *Nitzschia,* and *Thalassionema*, enhanced in the surface sediment in the southern stations (Fig. 3). Low nutrient conditions prevail in this region even during summer and winter monsoons. During the intermonsoon and premonsoon oligotrophy intensifies in these regions supporting the growth of smaller diatoms or non-diatoms (Garrison et al., 1998; Tarran et al., 1999; Chowdhury et al., 2021) that could sink slower compared to the larger cells in the north (Buesseler and Boyd, 2009).

Moreover, diatom frustules may dissolve while sinking and some of them (e. g. thickly silicified frustules) reach the abyssal plain and are preserved in the seafloor sediments. Nevertheless, the organic coating that protects siliceous frustules from dissolution (Lewin, 1961), can be degraded by heterotrophic bacterial activity (Bidle and Azam, 1999; Roubeix et al., 2008). The presence of OMZ in the northern stations (200–1200 m) could therefore slow down such dissolution facilitating frustules to reach the sea floor. On the other hand, in the south, small and thinly silicified diatom frustules (mostly due to DSi limitation) may be more fragile as they travel through the well-oxygenated water column and higher heterotrophic activity may enhance the risk of degradation leading to reduced frustules abundance on the seabed. In addition to this, the almost 700 m deeper water column in the south compared to the north could enhance the scope of degradation of sinking particles. This is consistent with our observation.

4.2.4 Zooplankton grazing

Two proxies representing zooplankton have been considered in this study 1) sterol biomarkers [cholesterol (Fig. 2i), and its degradative product cholestanol (Fig. 2j)], and 2) radiolarians (Fig. 2k). Cholesterol and cholestanol are produced in high amounts by zooplankton and are used as zooplankton proxies, nevertheless, some phytoplankton may also produce them in insignificant quantities (Kohlbach et al., 2021; Taipale et al., 2016; Wittenborn et al., 2020). Accordingly, the highest concentration of TOC-normalized cholesterol was found in the south indicating more zooplankton activity. In the RDA biplot, SST was grouped with cholestanol and was on the same side as cholesterol indicating higher zooplankton activity in the south. The association of TIC with cholesterol indicates that calcareous zooplankton could also be a source of cholesterol. Consequently, a higher fecal matter production could enhance particle flux compared to the north. Nonetheless, a major part of the fecal matter could also be degraded within the upper mesopelagic layer as reported by Iversen et al. (2017). In the Southern Ocean, more than 87% of fecal matter produced in the surface ocean can be lost via remineralization before reaching the upper mesopelagic zone (300 m) (Iversen et al. 2017). Likewise, the warmer temperature in the mesopelagic water column at our sampling locations could facilitate faster mineralization. Zooplankton grazing could largely alter the magnitude of carbon export flux (Moriceau et al., 2018). Thus, the low abundance of mesozooplankton within the OMZ may decrease defragmentation, which in turn slows down the bacterial remineralization of

phytodetritus allowing a higher amount of carbon to be exported to the abyssal plain (Cavan et al., 2017) (Fig. 5). Likewise, the lower zooplankton activity in the mesopelagic OMZ of the Arabian Sea (Wishner et al., 1998) may hinder particle fragmentation that usually accelerates degradation (Briggs et al., 2020). Similarly, at the northern stations, lower zooplankton abundance within the OMZ (Cavan et al., 2017) may restrict particle flux attenuation (Fig. 5).

In the western and central Arabian Sea, 50–100% of the diatom population can be grazed by copepods (Landry et al., 1998; Smith et al., 1998; Gauns et al., 2005). Importantly, diatom cell size can be a crucial factor that determines their grazing rates. Copepods exhibit the highest grazing rate when the ratio between prey and predator body size remains 18:1 on average (Hansen et al., 1994). In the north and at the axis of the Findlater Jet, the higher availability of nutrients, particularly DSi could promote large and thickly silicified diatoms which are difficult to graze for copepods (Hansen et al., 1994; Ryderheim et al., 2022). Subsequently, large centric diatoms like *Coscinodiscus radiatus* and *Rhizosolenia* spp. could escape grazing by copepods (Jansen, 2008; Löder et al., 2011) and can sink to the seafloor (Buesseler and Boyd, 2009; Kemp et al., 2006). On the contrary, the bloom-forming diatoms with thinly silicified frustules like *Chaetoceros* and *Leptocylindrus* (Sawant and Madhupratap, 1996; Chowdhury et al., 2021) can be grazed easily and are usually not found in the sediment. However, the lipid biomarkers of these diatoms (brassicasterol) may be preserved after transport through the water column in fecal pellets in surface sediments. In the case of the southern stations, smaller diatoms or non-diatoms could be consumed by microzooplankton (Swanberg and Anderson, 1985). Corroborating with this fact, the significantly higher number of radiolarians (Fig. 2k) which mostly consume smaller phytoplankton, bacterioplankton, and copepods (Caron et al., 1995) were higher in the south. A high abundance of radiolarians dominated by *Tetrapyle* sp. that are found under high salinity was also reported by a previous study from the Arabian Sea (Gupta, 2003).

4.3 Influence of lateral advection

Since there is evidence of advected waters reaching from the western Arabian Sea to its central part, the chances of particle transport also need to be considered. Stable nitrogen isotopic values of particulate organic matter ($\delta^{15}N_{POM,}$ Silori et al., 2021) revealed that nutrient enrichment mostly takes place via advection from the upwelling system as well as entrainment close to the axis of the Findlater Jet (16–18° N). Earlier studies also noticed the presence of slightly low saline waters in this region probably due to advection from the western Arabian Sea (Prasanna Kumar et al., 2000). Additionally, Silori et al. (2021) reported lower $\delta^{15}N$ values of particulate nitrogen during summer monsoon at the stations influenced by the axis suggesting laterally advected dissolved inorganic nitrogen from the Somali upwelling region. However, so far there is no report claiming that particulate organic matter can be advected such a long distance (~600 km) without being grazed/remineralized/sinking. Contrarily, there is plenty of evidence showing a direct relation between phytoplankton bloom and particle flux in these regions (Haake et al., 1993; Rixen et al., 2019a). Thus, the possibility of lateral transport of phytoplankton or detritus from the western Arabian Sea to the seabed of the central Arabian Sea may be overlain by vertical particle flux.

Conclusions

In our previous study (Pandey et al., 2023) using diatom frustules and sedimentary bulk parameters from the topmost part of the sediment core (0–0.5 cm), we established a link between the spatial trend in organic matter variability, atmospheric forcing, and phytoplankton

bloom. The present study aims for the first time to elucidate phytoplankton-driven particle flux to the seafloor using sedimentary lipid biomarkers from the central Arabian Sea. Such studies linking sedimentary organic matter to physical forcings and phytoplankton community have rarely been conducted in the central Arabian Sea. Importantly, most of the studies using sediment traps focused on diatoms and coccolithophores, but neglected dinoflagellates (Nair et al., 1989). A few studies proposed that the diatom blooms could be replaced by dinoflagellates. On the other hand, another study (Schubert et al., 1998), revealed that the relative contribution of dinosterol was higher than brassicasterol over the last 0.2 million years in this basin. Following this concept, we crosschecked the organic matter from the top 1 cm of surface sediments from more locations across a spatially variable transect (from high to low productive).

Our results indicated that dinoflagellates have contributed more to the sedimentary phytodetritus compared to diatoms even in the recent past. We propose that diatoms and coccolithophores do contribute to sedimentary particle flux. However, the dinoflagellates dominate due to their survival strategies during poor nutrient supply. We show that the distinct spatial variability in physical forcing drives the phytoplankton bloom and the particle flux is also closely coupled. Nevertheless, we also need to mention that the diatom community constructed from the frustules is not the direct producer of brassicasterol; the community provides more information about the surface oceanic processes including nutrient availability. The northernmost station in the central Arabian Sea was found to be a hotspot for sinking particles followed by subsequent preservation mostly due to the prevailing OMZ (Fig. 5). Both summer and winter monsoon-induced phytoplankton bloom dominated by diatoms led to the sinking of large thickly silicified frustules on the sediment floor. We hypothesized that the low oxygen within the thick OMZ could slow down the dissolution of frustules as well as heterotrophic degradation and fragmentation by zooplankton leading to low flux attenuation. Contrarily, in the south, higher dissolved oxygen levels could facilitate faster remineralization and higher zooplankton activity resulting in more flux attenuation and reduced particle transport to the sea floor. Contrary to the global scenario of expanding OMZs, a few recent studies (Vallivattathillam et al., 2023; Liu et al., 2024) showed that the southern part of the OMZ can get thinner in the future due to the higher supply of oxygen. Such changes could facilitate higher heterotrophic activities within the mesopelagic and thus could impact particle flux attenuation in this region and need to be investigated.

Acknowledgments

MP was supported by the Department of Science and Technology (DST) - Inspire Fellowship. This study is an outcome of the CSIR-NIO in-house program “Impact of Climate Change on the Physics, Biogeochemistry, and the Ecology of the North Indian Ocean (CliCNIO)” (MLP 1802) funded by the Council of Scientific and Industrial Research (CSIR). We express our gratitude to the captain, scientists, technical staff, ship cell staff, deckhands, and the students onboard *RV Sindhu Sadhana* (SSD 068) for their constant help and support during the cruise. We are thankful to the Director, CSIR NIO for his kind support. Ms. Teja Naik is acknowledged for her technical help in using the Coulometer under the central analytical facility in CSIR, NIO, Goa. The contribution number is XXXX. NB was funded by the Deutsche Forschungsgemeinschaft (DFG, German Research Foundation) under Germany‘s Excellence Strategy – EXC 2037 'CLICCS - Climate, Climatic Change, and Society' – Project Number: 390683824, contribution to the Center for Earth System Research and Sustainability (CEN) of Universität Hamburg. HB acknowledges the Humboldt Foundation for supporting her scientific visit to Hamburg University.

Availability of data and materials: The data are available online at Mendeley Data (DOI: 10.17632/xm4nxzdxb2.1)

Statements and Declarations

Competing Interests: *The authors have no relevant financial or non-financial interests to disclose.*

Ethical Approval: Not applicable

Consent to Participate: Not applicable

Consent to Publish: Not applicable

Authors' Contributions: *MP: Conceptualization, sampling, sample analysis; formal analysis, data curation, writing original manuscript and editing; HB: Conceptualization; Fund acquisition; sampling; manuscript reviewing and editing; DB: sampling; manuscript reviewing and editing NB: Sample analysis, Conceptualization; manuscript reviewing and editing BG: Conceptualization; reviewing and editing*

References

1. Abrantes, F.F.G. and Sancetta, C.: Diatom assemblages in surface sediments reflect coastal upwelling off southern Portugal, Oceanologica acta, 8,7–12, 1985.
2. Agustí, S. and Duarte, C.M.: Strong seasonality in phytoplankton cell lysis in the NW Mediterranean littoral, Limnology and Oceanography, 45, 940–947, https://doi.org/10.4319/lo.2000.45.4.0940, 2000.
3. Alonso-González, I.J., Arístegui, J., Lee, C., Sanchez-Vidal, A., Calafat, A., Fabrés, J., Sangrá, P., Masqué, P., Hernández-Guerra, A. and Benítez-Barrios, V.: Role of slowly settling particles in the ocean carbon cycle, Geophysical research letters, 37, https://doi.org/10.1029/2010GL043827, 2010.
4. Andruleit, H., Rogalla, U. and Stäger, S.: From living communities to fossil assemblages: origin and fate of coccolithophores in the northern Arabian Sea, Micropaleontology, 50, 5-21, https://doi.org/10.2113/50.Suppl_1.5, 2004.
5. Anju, M., Sreeush, M.G., Valsala, V., Smitha, B.R., Hamza, F., Bharathi, G. and Naidu, C.V.: Understanding the role of nutrient limitation on plankton biomass over Arabian Sea via 1-D coupled biogeochemical model and bio-Argo observations, Journal of Geophysical Research: Oceans, 125, e2019JC015502, https://doi.org/10.1029/2019JC015502, 2020.
6. Armbrecht, L.H., Lowe, V., Escutia, C., Iwai, M., McKay, R. and Armand, L.K.: Variability in diatom and silicoflagellate assemblages during mid-Pliocene glacial-interglacial cycles determined in Hole U1361A of IODP Expedition 318, Antarctic Wilkes Land Margin, Marine Micropaleontology, 139, 28–41, https://doi.org/10.1016/j.marmicro.2017.10.008, 2018.
7. Banse, K.: Seasonality of phytoplankton chlorophyll in the central and northern Arabian Sea, Deep Sea Research Part A, Oceanographic Research Papers, 34, 713–723, https://doi.org/10.1016/0198-0149(87)90032-X, 1987.
8. Banse, K., Naqvi, S.W.A., Narvekar, P.V., Postel, J.R. and Jayakumar, D.A.: Oxygen minimum zone of the open Arabian Sea: variability of oxygen and nitrite from daily to decadal timescales, Biogeosciences, 11, 2237–2261, https://doi.org/10.5194/bg-11-2237-2014, 2014.
9. Barnett, P.R.O., Watson, J. and Connelly, D.: A multiple corer for taking virtually undisturbed samples from shelf, bathyal and abyssal sediments, Oceanologica acta, 7, 399–408, 1984.

10. Bauer, S., Hitchcock, G.L., Olson, D.B.: Influence of monsoonally-forced Ekman dynamics upon surface layer depth and plankton biomass distribution in the Arabian Sea, Deep Sea Research, Part A Oceanographic Research Papers 38, 531–553, https://doi.org/10.1016/0198-0149(91)90062-K, 1991.
11. Behrenfeld, M.J., O'Malley, R.T., Siegel, D.A., McClain, C.R., Sarmiento, J.L., Feldman, G.C., Milligan, A.J., Falkowski, P.G., Letelier, R.M. and Boss, E.S.: Climate-driven trends in contemporary ocean productivity, Nature, 444,752–755, https://doi.org/10.1038/nature05317, 2006.
12. Bhattathiri, P.M.A., Pant, A., Sawant, S., Gauns, M., Matondkar, S.G.P. and Mohanraju, R.: Phytoplankton production and chlorophyll, Current Science, 71, 1996.
13. Bidle, K.D. and Azam, F.: Accelerated dissolution of diatom silica by marine bacterial assemblages, Nature, 397, 508–512, https://doi.org/10.1038/17351, 1999.
14. Boyd, P.W. and Newton, P.P.: Does planktonic community structure determine downward particulate organic carbon flux in different oceanic provinces?, Deep Sea Research Part I: Oceanographic Research Papers, 46, 63–91, https://doi.org/10.1016/S09670637(98)00066-1, 1999.
15. Brassell, S.C., Brereton, R.G., Eglinton, G., Grimalt, J., Liebezeit, G., Marlowe, I.T., Pflaumann, U. and Sarnthein, M.: Palaeoclimatic signals recognized by chemometric treatment of molecular stratigraphic data, Organic Geochemistry, 10(4-6), 649–660, https://doi.org/10.1016/S0146-6380(86)80001-8, 1986.
16. Briggs, N., Dall'Olmo, G. and Claustre, H.: Major role of particle fragmentation in regulating biological sequestration of CO_2 by the oceans, Science, 367, 791–793, https://doi.org/10.1126/science.aay1790, 2020.
17. Buesseler, K.O. and Boyd, P.W.: Shedding light on processes that control particle export and flux attenuation in the twilight zone of the open ocean, Limnology and Oceanography, 54, 1210–1232, https://doi.org/10.4319/lo.2009.54.4.1210, 2009.
18. Buesseler, K.O.: The decoupling of production and particulate export in the surface ocean, Global Biogeochemical Cycles, 12, 297–310, https://doi.org/10.1029/97GB03366, 1998.
19. Cabrera-Brufau, M., Arin, L., Sala, M.M., Cermeño, P. and Marrasé, C.: Diatom dominance enhances resistance of phytoplanktonic POM to mesopelagic microbial decomposition, Frontiers in Marine Science, 8, p.683354, https://doi.org/10.3389/fmars.2021.683354, 2021.
20. Caron, D.A., Michaels, A.F., Swanberg, N.R. and Howse, F.A.: Primary productivity by symbiont-bearing planktonic sarcodines (Acantharia, Radiolaria, Foraminifera) in surface waters near Bermuda, Journal of Plankton Research, 17, 103–129. https://doi.org/10.1093/plankt/17.1.103, 1995.
21. Cavan, E.L., Trimmer, M., Shelley, F. and Sanders, R.: Remineralization of particulate organic carbon in an ocean oxygen minimum zone. Nature Communications, 8(1), p.14847, https://doi.org/10.1038/ncomms14847, 2017.
22. Chowdhury, M., Biswas, H., Mitra, A., Silori, S., Sharma, D., Bandyopadhyay, D., Shaik, A.U.R., Fernandes, V. and Narvekar, J.: Southwest monsoon-driven changes in the phytoplankton community structure in the central Arabian Sea (2017–2018): After two decades of JGOFS, Progress in Oceanography, 197, p.102654, https://doi.org/10.1016/j.pocean.2021.102654, 2021.
23. Chowdhury, M., Biswas, H., Silori, S. and Sharma, D.: Spatiotemporal variability in phytoplankton size class modulated by summer monsoon wind forcing in the central Arabian Sea, Journal of Geophysical Research: Oceans, 129, e2023JC019880, https://doi.org/10.1029/2023JC019880, 2024.

24. Copernicus Climate Change Service (C3S), ERA5: Fifth generation of ECMWF atmospheric reanalyses of the global climate, Copernicus Climate Change Service Climate Data Store (CDS), 2017.
25. Desikachary, T.V.: Atlas of Diatoms (Marine Diatoms of the Indian Ocean Region), 6, Madras Science Foundation, Madras Fasc, 1–13, 1989.
26. Ding, Y., Bi, R., Sachs, J., Chen, X., Zhang, H., Li, L. and Zhao, M., Lipid biomarker production by marine phytoplankton under different nutrient and temperature regimes. Organic Geochemistry, 131, 34-49. https://doi.org/10.1016/j.orggeochem.2019.01.008, 2019.
27. Eglinton, T.I. and Eglinton, G., 2008. Molecular proxies for paleoclimatology, Earth and Planetary Science Letters, 275(1–2), 1–16, https://doi.org/10.1016/j.epsl.2008.07.012, 2008.
28. Engel, A., Wagner, H., Le Moigne, F.A. and Wilson, S.T.: Particle export fluxes to the oxygen minimum zone of the eastern tropical North Atlantic, Biogeosciences, 14,1825-1838, https://doi.org/10.5194/bg-14-1825-2017, 2017.
29. Field, C.B., Behrenfeld, M.J., Randerson, J.T. and Falkowski, P.: Primary production of the biosphere: integrating terrestrial and oceanic components, Science, 281, 237–240, https://doi.org/10.1126/science.281.5374.237, 1998.
30. Findlater, J.: Mean monthly airflow at low levels over the western Indian Ocean (No. 116). HM Stationery Office, Pure Appl. Geophys. PAGEOPH 115, 1251–1262, https://doi.org/10.1007/BF00874408, 1971.
31. Francois, R., Honjo, S., Krishfield, R. and Manganini, S.: Factors controlling the flux of organic carbon to the bathypelagic zone of the ocean, Global Biogeochemical Cycles, 16, 34–1, https://doi.org/10.1029/2001GB001722, 2002.
32. García-Oliva, O., Hantzsche, F.M., Boersma, M. and Wirtz, K.W.: Phytoplankton and particle size spectra indicate intense mixotrophic dinoflagellates grazing from summer to winter. Journal of Plankton Research, 44, 224–240, https://doi.org/10.1093/plankt/fbac013, 2022.
33. Garrison, D.L., Gowing, M.M. and Hughes, M.P.: Nano-and microplankton in the northern Arabian Sea during the Southwest Monsoon, August–September 1995 A US–JGOFS study, Deep Sea Research Part II: Topical Studies in Oceanography, 45, 2269–2299, https://doi.org/10.1016/S0967-0645(98)00071-X, 1998.
34. Gauns, M., Madhupratap, M., Ramaiah, N., Jyothibabu, R., Fernandes, V., Paul, J.T. and Kumar, S.P.: Comparative accounts of biological productivity characteristics and estimates of carbon fluxes in the Arabian Sea and the Bay of Bengal. Deep Sea Research Part II: Topical Studies in Oceanography, 52, 2003–2017, https://doi.org/10.1016/j.dsr2.2005.05.009, 2005.
35. Glibert, P.M., Wilkerson, F.P., Dugdale, R.C., Raven, J.A., Dupont, C.L., Leavitt, P.R., Parker, A.E., Burkholder, J.M. and Kana, T.M.: Pluses and minuses of ammonium and nitrate uptake and assimilation by phytoplankton and implications for productivity and community composition, with emphasis on nitrogen-enriched conditions, Limnology and Oceanography, 61, 165–197, https://doi.org/10.1002/lno.10203, 2016.
36. Gupta, S.M.: Orbital frequencies in radiolarian assemblages of the central Indian Ocean: implications on the Indian summer monsoon, Palaeogeography, Palaeoclimatology, Palaeoecology, 197(1-2), 97–112, https://doi.org/10.1016/S0031-0182(03)00388-2, 2003.
37. Haake, B., Ittekkot, V., Rixen, T., Ramaswamy, V., Nair, R.R. and Curry, W.B.: Seasonality and interannual variability of particle fluxes to the deep Arabian Sea, Deep Sea Research Part I: Oceanographic Research Papers, 40(7), 1323–1344, https://doi.org/10.1016/0967-0637(93)90114-I, 1993.

38. Hansen, B., Bjornsen, P.K. and Hansen, P.J.: The size ratio between planktonic predators and their prey, Limnology and oceanography, 39(2), 395–403, https://doi.org/10.4319/lo.1994.39.2.0395, 1994.
39. Hu, L., Liu, Y., Xiao, X., Gong, X., Zou, J., Bai, Y., Gorbarenko, S., Fahl, K., Stein, R. and Shi, X.: Sedimentary records of bulk organic matter and lipid biomarkers in the Bering Sea: A centennial perspective of sea-ice variability and phytoplankton community, Marine Geology, 429, 106308, https://doi.org/10.1016/j.margeo.2020.106308 , 2020.
40. Iversen, M.H., Pakhomov, E.A., Hunt, B.P., Van der Jagt, H., Wolf-Gladrow, D. and Klaas, C.: Sinkers or floaters? Contribution from salp pellets to the export flux during a large bloom event in the Southern Ocean, Deep Sea Research Part II: Topical Studies in Oceanography, 138, 116–125, https://doi.org/10.1016/j.dsr2.2016.12.004, 2017.
41. Iversen, M.H.: Carbon Export in the Ocean: A Biologist's Perspective, Annual Review of Marine Science, 15, 357–381, 10.1146/annurev-marine-032122-035153, 2023.
42. Jaramillo-Madrid, A.C., Ashworth, J., Fabris, M. and Ralph, P.J., Phytosterol biosynthesis and production by diatoms (Bacillariophyceae). Phytochemistry, 163.46-57. https://doi.org/10.1016/j.phytochem.2019.03.018, 2019.
43. Jaramillo-Madrid A.C., Ashworth, J., Ralph, P. J., Levels of Diatom Minor Sterols Respond to Changes in Temperature and Salinity. Journal of Marine Science and Engineering. 8(2), 85, https://doi.org/10.3390/jmse8020085, 2020.
44. Jansen, S.: Copepods grazing on Coscinodiscus wailesii: a question of size?, Helgoland Marine Research, 62(3), 251–255, https://doi.org/10.1007/s10152-008-0113-z, 2008.
45. Kohlbach, D., Hop, H., Wold, A., Schmidt, K., Smik, L., Belt, S. T., Keck, Al-Habahbeh, A., Woll, M, Graeve, M., Dąbrowska, A. M,s Tatarek, A., Atkinson, A., and Assmy, P.: Multiple Trophic Markers Trace Dietary Carbon Sources in Barents Sea Zooplankton During Late Summer. Front. Mar. Sci. 7:610248. doi: 10.3389/fmars.2020.610248, 2021.
46. Keil, R.G., Neibauer, J.A., Biladeau, C., van der Elst, K. and Devol, A.H.: A multiproxy approach to understanding the" enhanced" flux of organic matter through the oxygen-deficient waters of the Arabian Sea, Biogeosciences, 13(7), 2077–2092, https://doi.org/10.5194/bg-13-2077-2016, 2016.
47. Kemp, A.E., Pearce, R.B., Grigorov, I., Rance, J., Lange, C.B., Quilty, P. and Salter, I., Production of giant marine diatoms and their export at oceanic frontal zones: Implications for Si and C flux from stratified oceans, Global Biogeochemical Cycles, 20(4), https://doi.org/10.1029/2006GB002698, 2006.
48. Krause, J.W., Schulz, I.K., Rowe, K.A., Dobbins, W., Winding, M.H., Sejr, M.K., Duarte, C.M. and Agustí, S.: Silicic acid limitation drives bloom termination and potential carbon sequestration in an Arctic bloom, Scientific Reports, 9(1), 8149, https://doi.org/10.1038/s41598-019-44587-4, 2019.
49. Landry, M.R., Brown, S.L., Campbell, L., Constantinou, J. and Liu, H.: Spatial patterns in phytoplankton growth and microzooplankton grazing in the Arabian Sea during monsoon forcing, Deep Sea Research Part II: Topical Studies in Oceanography, 45(10–11), 2353–2368, https://doi.org/10.1016/S0967-0645(98)00074-5, 1998.
50. Latasa, M. and Bidigare, R.R.: A comparison of phytoplankton populations of the Arabian Sea during the Spring Intermonsoon and Southwest Monsoon of 1995 as described by HPLC-analyzed pigments, Deep Sea Research Part II: Topical Studies in Oceanography, 45(10-11), 2133–2170, https://doi.org/10.1016/S0967-0645(98)00066-6, 1998.
51. Le Moigne, F.A.: Pathways of organic carbon downward transport by the oceanic biological carbon pump, Frontiers in Marine Science, 6, 634, https://doi.org/10.3389/fmars.2019.00634, 2019.

52. Lewin, J.C.: The dissolution of silica from diatom walls, Geochimica et Cosmochimica Acta, 21(3-4), 182–198, https://doi.org/10.1016/S0016-7037(61)80054-9, 1961.
53. Liu, D., Shen, X., Di, B., Shi, Y., Keesing, J.K., Wang, Y. and Wang, Y.: Palaeoecological analysis of phytoplankton regime shifts in response to coastal eutrophication, Marine Ecology Progress Series, 475, 1–14, https://doi.org/10.3354/meps10234, 2013.
54. Liu, T., Qiu, Y., Lin, X., Ni, X., Wang, L., Li, H. and Jing, C., Dissolved oxygen recovery in the oxygen minimum zone of the Arabian Sea in recent decade as observed by BGC-argo floats. Geophysical Research Letters, 51(12), p.e2024GL108841. https://doi.org/10.1029/2024GL108841, 2024
55. Löder, M.G., Meunier, C., Wiltshire, K.H., Boersma, M. and Aberle, N.: The role of ciliates, heterotrophic dinoflagellates and copepods in structuring spring plankton communities at Helgoland Roads, North Sea, Marine biology, 158, 1551–1580, https://doi.org/10.1007/s00227-011-1670-2, 2011.
56. Madhupratap, M., Kumar, S.P., Bhattathiri, P.M.A., Kumar, M.D., Raghukumar, S., Nair, K.K.C. and Ramaiah, N.: Mechanism of the biological response to winter cooling in the northeastern Arabian Sea, Nature, 384(6609), 549–552, https://doi.org/10.1038/384549a0, 1996.
57. Marsay, C.M., Sanders, R.J., Henson, S.A., Pabortsava, K., Achterberg, E.P. and Lampitt, R.S.: Attenuation of sinking particulate organic carbon flux through the mesopelagic ocean, Proceedings of the National Academy of Sciences, 112(4), 1089–1094, https://doi.org/10.1073/pnas.14153111, 2015.
58. McCreary, J.P., Murtugudde, R., Vialard, J., Vinayachandran, P.N., Wiggert, J.D., Hood, R.R., Shankar, D. and Shetye, S.: Biophysical processes in the Indian Ocean, Indian Ocean biogeochemical processes and ecological variability, 185, 9–32, https://doi.org/10.1029/2008GM000768, 2009.
59. Mergulhao, L.P., Mohan, R., Murty, V.S.N., Guptha, M.V.S. and Sinha, D.K.: Coccolithophores from the central Arabian Sea: Sediment trap results, Journal of earth system science, 115, 415–428, https://doi.org/10.1007/BF02702870, 2006.
60. Meyers, P.A.: Organic geochemical proxies of paleoceanographic, paleolimnologic, and paleoclimatic processes, Organic geochemistry, 27(5–6), 213–250, https://doi.org/10.1016/S0146-6380(97)00049-1, 1997.
61. Moriceau, B., Iversen, M.H., Gallinari, M., Evertsen, A.J.O., Le Goff, M., Beker, B., Boutorh, J., Corvaisier, R., Coffineau, N., Donval, A. and Giering, S.L., Copepods boost the production but reduce the carbon export efficiency by diatoms, Frontiers in Marine Science, 5, 82, https://doi.org/10.3389/fmars.2018.00082, 2018.
62. Müller, J., Wagner, A., Fahl, K., Stein, R., Prange, M. and Lohmann, G.: Towards quantitative sea ice reconstructions in the northern North Atlantic: A combined biomarker and numerical modelling approach, Earth and Planetary Science Letters, 306(3-4), 137–148, https://doi.org/10.1016/j.epsl.2011.04.011, 2011.
63. Nair, R.R., Ittekkot, V., Manganini, S.J., Ramaswamy, V., Haake, B., Degens, E.T., Desai, B.T. and Honjo, S.: Increased particle flux to the deep ocean related to monsoons, Nature, 338(6218), 749–751, https://doi.org/10.1038/338749a0, 1989.
64. Nomaki, H., Rastelli, E., Ogawa, N.O., Matsui, Y., Tsuchiya, M., Manea, E., Corinaldesi, C., Hirai, M., Ohkouchi, N., Danovaro, R. and Nunoura, T.: In situ experimental evidences for responses of abyssal benthic biota to shifts in phytodetritus compositions linked to global climate change, Global Change Biology, 27(23), 6139–6155, https://doi.org/10.1111/gcb.15882, 2021.
65. Pandey, M., Biswas, H. and Chowdhury, M.: Interlinking diatom frustule diversity from the abyss of the central Arabian Sea to surface processes: physical forcing and oxygen

minimum zone, Environmental Monitoring and Assessment, 195(1), 161, https://doi.org/10.1007/s10661-022-10749-7, 2023.
66. Pandey, M. and Biswas, H.: May. An account of the key diatom frustules from the surface sediments of the Central and Eastern Arabian Sea and their biogeochemical significance, In EGU General Assembly Conference Abstracts (EGU-131), https://doi.org/10.5194/egusphere-egu23-131, 2023.
67. Pandey, Medhavi; Biswas, Haimanti; Birgel, Daniel; Burdanowitz, Nicole; Gaye, Birgit, "Understanding biological carbon pump in the central Arabian Sea using phytoplankton biomarkers and diatom frustules from surface sediments.", Mendeley Data, V1, doi: 10.17632/xm4nxzdxb2.1, 2024.
68. Peng, P., Bi, R., Sachs, J.P., Shi, J., Luo, Y., Chen, W., Huh, C.A., Yu, M., Cao, Y., Wang, Y. and Cao, Z.: Phytoplankton community changes in a coastal upwelling system during the last century, Global and Planetary Change, 224, 104101, https://doi.org/10.1016/j.gloplacha.2023.104101, 2023.
69. Prahl, F. G., Muehlhausen, L. A. and Zahnle, D. L.: Further evaluation of long-chain alkenones as indicators of paleoceanographic conditions, Geochim. Cosmochim. Acta, 52(9), 2303–2310, doi:10.1016/0016-7037(88)90132-9, 1988.
70. Prahl, F.G., Dymond, J. and Sparrow, M.A.: Annual biomarker record for export production in the central Arabian Sea, Deep Sea Research Part II: Topical Studies in Oceanography, 47(7-8), 1581–1604, https://doi.org/10.1016/S0967-0645(99)00155-1, 2000.
71. Prahl, F.G. and Wakeham, S.G.: Calibration of unsaturation patterns in long-chain ketone compositions for palaeotemperature assessment, Nature, 330(6146), pp.367-369, https://doi.org/10.1038/330367a0, 1987.
72. Prasanna Kumar S., Madhupratap, M., Kumar, M.D., Gauns, M., Muraleedharan, P.M., Sarma, V.V.S.S. and De Souza, S.N.: Physical control of primary productivity on a seasonal scale in central and eastern Arabian Sea, Journal of Earth System Science, 109, 433–441, https://doi.org/10.1007/BF02708331, 2000.
73. Prasanna Kumar. S., and Narvekar, J.: Seasonal variability of the mixed layer in the central Arabian Sea and its implication on nutrients and primary productivity, Deep Sea Research Part II: Topical Studies in Oceanography, 52(14-15), 1848–1861, https://doi.org/10.1016/j.dsr2.2005.06.002, 2005.
74. Prasanna Kumar. S., Ramaiah, N., Gauns, M., Sarma, V.V.S.S., Muraleedharan, P.M., Raghukumar, S., Kumar, M.D. and Madhupratap, M.: Physical forcing of biological productivity in the Northern Arabian Sea during the Northeast Monsoon, Deep Sea Research Part II: Topical Studies in Oceanography, 48(6-7), 1115–1126, https://doi.org/10.1016/S0967-0645(00)00133-8, 2001.
75. Ragueneau, O., Schultes, S., Bidle, K., Claquin, P. and Moriceau, B.: Si and C interactions in the world ocean: Importance of ecological processes and implications for the role of diatoms in the biological pump, Global Biogeochemical Cycles, 20(4), https://doi.org/10.1029/2006GB002688, 2006.
76. Rixen, T., Gaye, B. and Emeis, K.C.: The monsoon, carbon fluxes, and the organic carbon pump in the northern Indian Ocean, Progress in oceanography, 175, 24–39, https://doi.org/10.1016/j.pocean.2019.03.001, 2019a.
77. Rixen, T., Gaye, B., Emeis, K.C. and Ramaswamy, V.: The ballast effect of lithogenic matter and its influences on the carbon fluxes in the Indian Ocean, Biogeosciences, 16(2), 485–503, https://doi.org/10.5194/bg-16-485-2019, 2019b.
78. Rodríguez-Miret, X., del Carmen Trapote, M., Sigró, J. and Vegas-Vilarrúbia, T.: Diatom responses to warming, heavy rains and human impact in a Mediterranean lake since the preindustrial period, Science of The Total Environment, 884, 163685, https://doi.org/10.1016/j.scitotenv.2023.163685, 2023.

79. Roubeix, V., Becquevort, S. and Lancelot, C.: Influence of bacteria and salinity on diatom biogenic silica dissolution in estuarine systems, Biogeochemistry, 88, 47–62, https://doi.org/10.1007/s10533-008-9193-8, 2008.
80. Roxy, M. K., Modi, A., Murtugudde, R., Valsala, V., Panickal, S., Kumar, S. P., Ravichandran, M., Vichi, M., and Levy, M.: A reduction in marine primary productivity driven by rapid warming over the tropical Indian Ocean, Geophysical Research Letters, 43, 826–833, https://doi.org/10.1002/2015GL066979, 2016.
81. Ryderheim, F., Grønning, J. and Kiørboe, T.: Thicker shells reduce copepod grazing on diatoms, Limnology and Oceanography Letters, 7(5), 435–442, https://doi.org/10.1002/lol2.10243, 2022.
82. Sawant, S. and Madhupratap, M.: Seasonality and composition of phytoplankton. Current Science, 71(11), 1996.
83. Schiebel, R., Zeltner, A., Treppke, U. F., Waniek, J. J., Bollmann, J., Rixen, T., & Hemleben, C.. Distribution of diatoms, coccolithophores and planktic foraminifers along a trophic gradient during SW monsoon in the Arabian Sea. *Marine* Micropaleontology, 51(3-4), 345-371. http://dx.doi.org/10.1016/j.marmicro.2004.02.001, 2004.
84. Schubert, C.J., Villanueva, J., Calvert, S.E., Cowie, G.L., Von Rad, U., Schulz, H., Berner, U. and Erlenkeuser, H.: Stable phytoplankton community structure in the Arabian Sea over the past 200,000 years, Nature, 394(6693), 563–566, https://doi.org/10.1038/29047, 1998.
85. Schulte, S., Mangelsdorf, K. and Rullkötter, J.: Organic matter preservation on the Pakistan continental margin as revealed by biomarker geochemistry, Organic Geochemistry, 31(10), 1005–1022, https://doi.org/10.1016/S0146-6380(00)00108-X, 2000.
86. Schulte, S., Rostek, F., Bard, E., Rullkötter, J. and Marchal, O.: Variations of oxygen-minimum and primary productivity recorded in sediments of the Arabian Sea, Earth and Planetary Science Letters, 173(3), 205–221, https://doi.org/10.1016/S0012-821X(99)00232-0, 1999.
87. Sharma, S., Ha, K.-J., Yamaguchi, R., Rodgers, K. B., Timmermann, A., and Chung, E.: Future Indian Ocean warming patterns, Nature Communications, 14, 1789, https://doi.org/10.1038/s41467-023-37435-7, 2023
88. Silori, S., Sharma, D., Chowdhury, M., Biswas, H., Cardinal, D. and Mandeng-Yogo, M.: Particulate organic matter dynamics and its isotopic signatures (δ13CPOC and δ15NPN) in relation to physical forcing in the central Arabian Sea during SW monsoon (2017–2018), Science of the Total Environment, 785, 147326, https://doi.org/10.1016/j.scitotenv.2021.147326, 2021.
89. Singh, U.B. and Ahluwalia, A.S.: Microalgae: a promising tool for carbon sequestration, Mitigation and Adaptation Strategies for Global Change, 18(1), 73–95, https://doi.org/10.1007/s11027-012-9393-3, 2013.
90. Smayda, T.J. and Reynolds, C.S.: Community assembly in marine phytoplankton: application of recent models to harmful dinoflagellate blooms, Journal of plankton research, 23(5), 447–461, https://doi.org/10.1093/plankt/23.5.447, 2001.
91. Smetacek, V.S.: Role of sinking in diatom life-history cycles: ecological, evolutionary and geological significance, Marine biology, 84, 239–251, https://doi.org/10.1007/BF00392493, 1985.
92. Smith, S., Roman, M., Prusova, I., Wishner, K., Gowing, M., Codispoti, L.A., Barber, R., Marra, J. and Flagg, C.: Seasonal response of zooplankton to monsoonal reversals in the Arabian Sea, Deep Sea Research Part II: Topical Studies in Oceanography, 45(10-11), 2369–2403, https://doi.org/10.1016/S0967-0645(98)00075-7, 1998.

93. Sonzogni, C., Bard, E., Rostek, F., Lafont, R., Rosell-Mele, A. and Eglinton, G.: Core-top calibration of the alkenone index vs sea surface temperature in the Indian Ocean, Deep Sea Res. Part II Top. Stud. Oceanogr., 44(6), 1445–1460, doi:10.1016/S0967-0645(97)00010-6, 1997.
94. Stoecker, D.K.: Mixotrophy among Dinoflagellates 1. Journal of eukaryotic microbiology, 46, 397-401, https://doi.org/10.1111/j.1550-7408.1999.tb04619.x, 1999.
95. Stoecker, D.K., Hansen, P.J., Caron, D.A. and Mitra, A.: Mixotrophy in the marine plankton, Annual Review of Marine Science, 9, 311–335, https://doi.org/10.1146/annurev-marine-010816-060617, 2017.
96. Swanberg, N. R., and Anderson, O.R.: The nutrition of radiolarians: Trophic activity of some solitary Spumellaria 1, Limnology and Oceanography, 30, 646–652, https://doi.org/10.4319/lo.1985.30.3.0646, 1985.
97. Taipale, S. J., Hiltunen, M, Vuorio, K., and Peltomaa, E., Suitability of Phytosterols Alongside Fatty Acids as Chemotaxonomic Biomarkers for Phytoplankton. Front. Plant Sci. 7:212. doi: 10.3389/fpls.2016.00212, 2016.
98. Tarran, G.A., Burkill, P.H., Edwards, E.S. and Woodward, E.M.S.: Phytoplankton community structure in the Arabian Sea during and after the SW monsoon, 1994, Deep Sea Research Part II: Topical Studies in Oceanography, 46, 655–676, https://doi.org/10.1016/S0967-0645(98)00122-2, 1999.
99. Ter Braak, C.J. and Smilauer, P.: CANOCO reference manual and CanoDraw for Windows user's guide: software for canonical community ordination (version 4.5), www. canoco. com, 2002.
100. Tomas, C. R., (Ed.), Identifying marine phytoplankton. Elsevier, 1997.
101. Tréguer, P., Bowler, C., Moriceau, B., Dutkiewicz, S., Gehlen, M., Aumont, O., Bittner, L., Dugdale, R., Finkel, Z., Iudicone, D. and Jahn, O.: Influence of diatom diversity on the ocean biological carbon pump, Nature Geoscience, 11, 27–37, https://doi.org/10.1038/s41561-017-0028-x, 2018.
102. Vallivattathillam, P., Lachkar, Z. and Lévy, M.: Shrinking of the Arabian Sea oxygen minimum zone with climate change projected with a downscaled model, Frontiers in Marine Science, 10, 1123739, https://doi.org/10.3389/fmars.2023.1123739, 2023.
103. Véron, B., Dauguet, J. C., and Billard, C. Sterolic biomarkers in marine phytoplankton. II. Free and conjugated sterols of seven species used in mariculture. Journal of phycology, 34(2), 273-279. https://doi.org/10.1046/j.1529-8817.1998.340273.x, 1998.
104. Volk, T. and Hoffert, M.I.: Ocean carbon pumps: Analysis of relative strengths and efficiencies in ocean-driven atmospheric CO_2 changes, The carbon cycle and atmospheric CO2: Natural variations Archean to present, 32, 99–110, https://doi.org/10.1029/GM032p0099, 1985.
105. Volkman, J.K., Barrett, S.M., Blackburn, S.I., Mansour, M.P., Sikes, E.L. and Gelin, F.: Microalgal biomarkers: a review of recent research developments. Organic Geochemistry, 29(5-7), 1163-1179, https://doi.org/10.1016/S0146-6380(98)00062-X, 1998.
106. Volkman, J.: Sterols in microorganisms. Applied microbiology and Biotechnology, 60, 495-506, https://doi.org/10.1007/s00253-002-1172-8 , 2003.
107. Wakeham, S.G., Peterson, M.L., Hedges, J.I. and Lee, C.: Lipid biomarker fluxes in the Arabian Sea, with a comparison to the equatorial Pacific Ocean. Deep Sea Research Part II: Topical Studies in Oceanography, 49, 2265–2301, https://doi.org/10.1016/S0967-0645(02)00037-1, 2002.
108. Ward, B.B., Devol, A.H., Rich, J.J., Chang, B.X., Bulow, S.E., Naik, H., Pratihary, A. and Jayakumar, A.: Denitrification as the dominant nitrogen loss process in the Arabian Sea, Nature, 461, 78–81, https://doi.org/10.1038/nature08276, 2009.

109. Wishner, K.F., Gowing, M.M. and Gelfman, C.: Mesozooplankton biomass in the upper 1000 m in the Arabian Sea: overall seasonal and geographic patterns, and relationship to oxygen gradients, Deep Sea Research Part II: Topical Studies in Oceanography, 45, 2405–2432, https://doi.org/10.1016/S0967-0645(98)00078-2, 1998.
110. Wittenborn, A.K., Schmale, O. and Thiel, V.: Zooplankton impact on lipid biomarkers in water column vs. surface sediments of the stratified Eastern Gotland Basin (Central Baltic Sea), Plos one, 15, e0234110, https://doi.org/10.1371/journal.pone.0234110, 2020.
111. Xiong, W., Mei, X., Meng, X., Chen, H. and Yang, H.: Phytoplankton biomarkers in surface sediments from Liaodong Bay and their potential as indicators of primary productivity, Marine Pollution Bulletin, 159, 111536, https://doi.org/10.1016/j.marpolbul.2020.111536, 2020.
112. Zúñiga, D., Sanchez-Vidal, A., Flexas, M.D.M., Carroll, D., Rufino, M.M., Spreen, G., Calafat, A. and Abrantes, F.: Sinking diatom assemblages as a key driver for deep carbon and silicon export in the Scotia Sea (Southern Ocean), Frontiers in Earth Science, 9, 579198, https://doi.org/10.3389/feart.2021.579198, 2021.

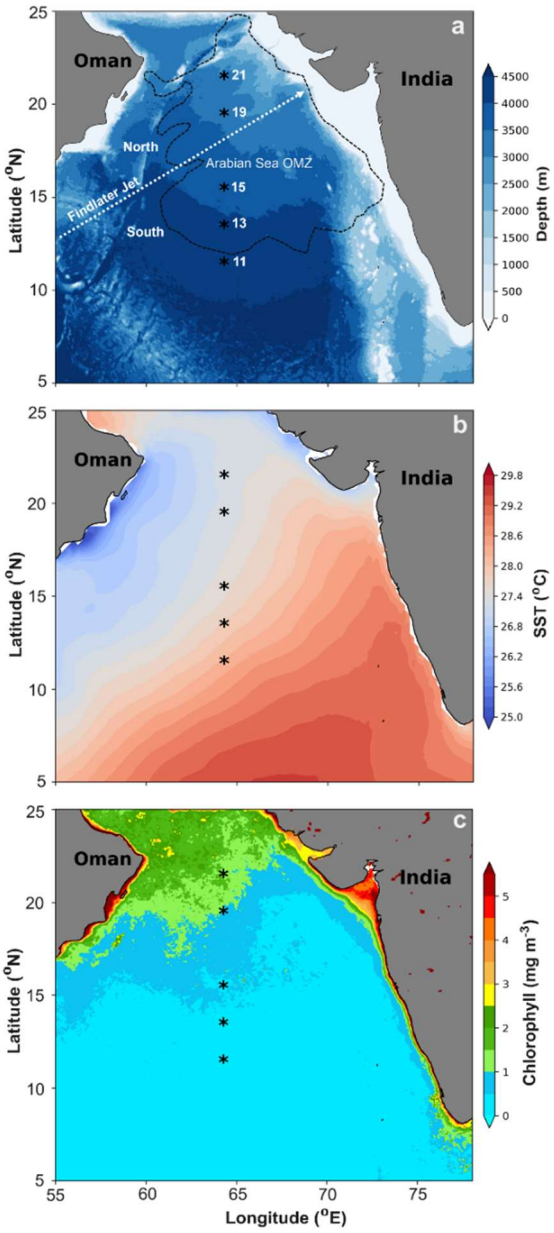

Figure 1. a) Map showing the study locations in the Central Arabian Sea along 64° E transect during SSD-068 (Dec 2019). The low-level atmospheric jet (Findlater Jet) is depicted in white dashed arrow and the boundary of the Oxygen Minimum Zone (OMZ) (0.5 mmol L^{-1} O_2 concentration) is displayed in the black dashed line; b) average SST (2017-2020) values depicting spatial variability among the sampling stations from the north to south; c) average Chl*a* values derived from the satellite for the period 2017-2020 over the Arabian sea, indicating average phytoplankton biomass remains higher on an annual scale for the stations in the north compared to the south.

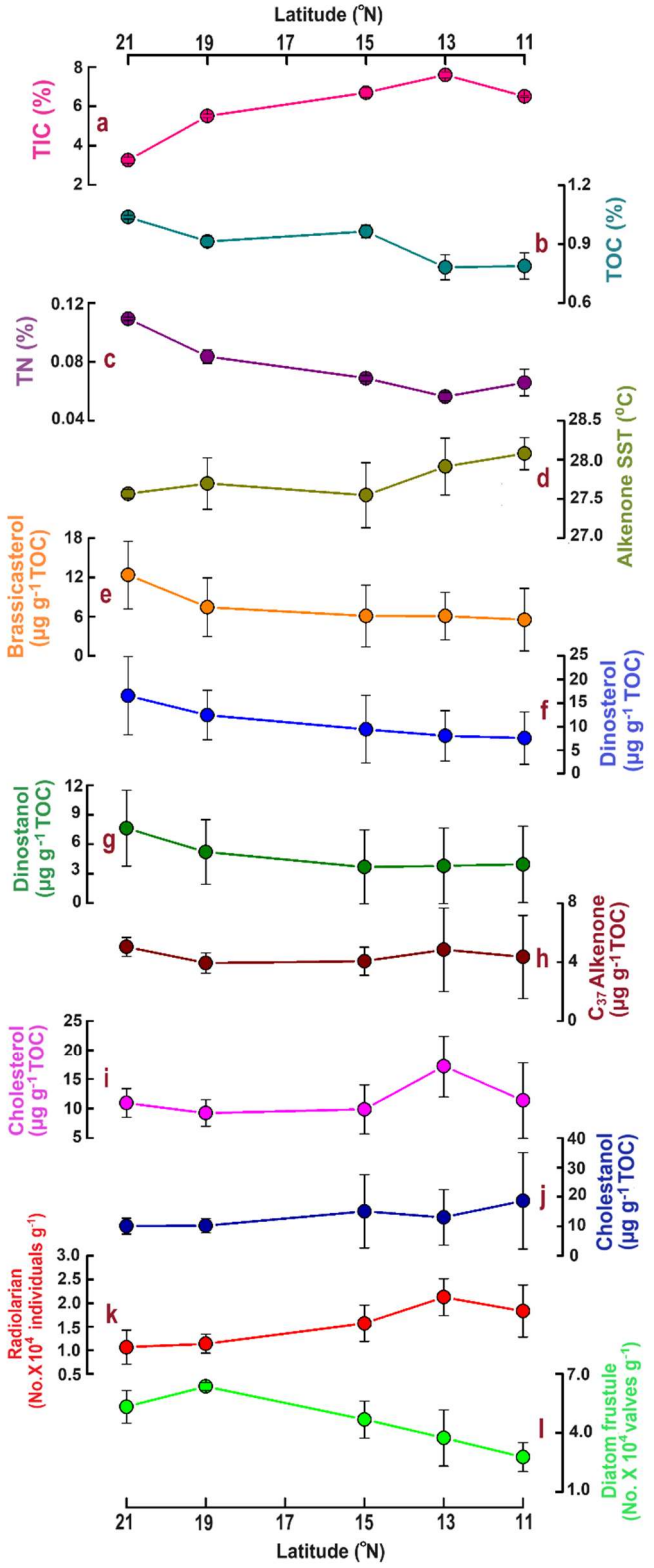

Figure 2. The distribution of total inorganic carbon (TIC %) (a), total organic carbon (TOC %) (b), total nitrogen (TN%) (c), alkenone based sea surface temperature (SST °C) (d), brassicasterol (e), dinosterol (f), dinostanol (g), C_{37} alkenones (h), cholesterol (i), cholestanol (j), radiolarians (k), and diatom frustules (l) along the 64° E transect in the central Arabian Sea.

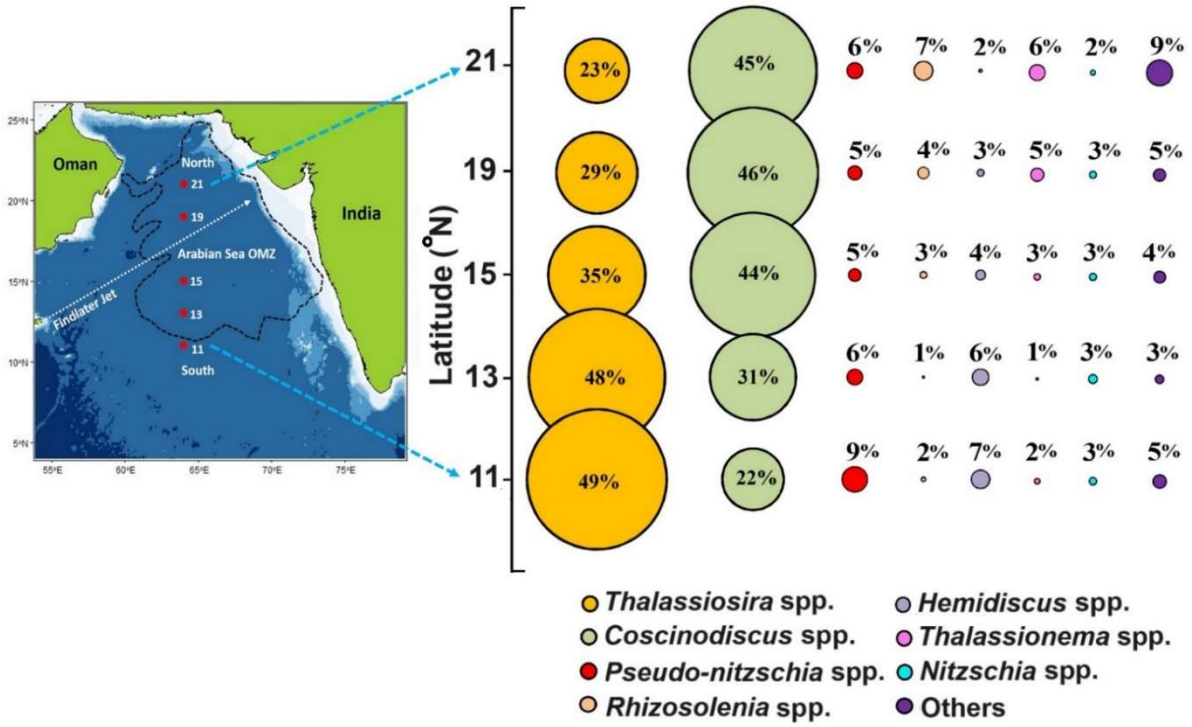

Figure 3. The bubble plot shows the relative percentage of diatom frustules of major species (>3% of total abundance) from surface sediment samples (average of 0 – 0.5 cm and 0.5 - top 1 cm) along the 64° E transect in the central Arabian Sea. Individual contributions from centric and pennate diatoms <3% were summed as "others". The colors denote the specific phytoplankton taxa as indicated by colored closed circles at the bottom of the panel.

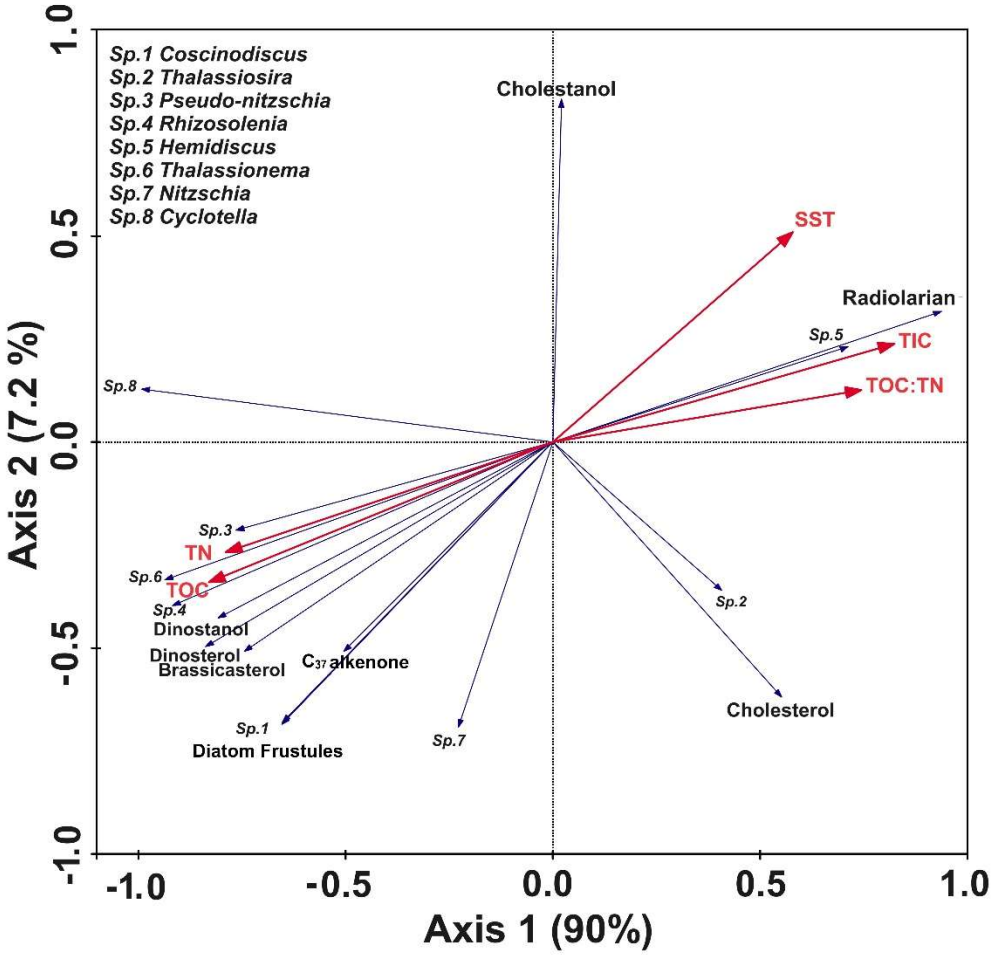

Figure 4. RDA biplot shows the interrelationship between the key parameters shown in blue (diatom frustules, biomarkers, radiolarians) and bulk sedimentary parameters indicated in red (TOC; TN, TIC, TOC: TN; SST). The names of diatoms genera are marked as "Sp." and are mentioned in the top left side of the panel**.** Axis 1 and axis 2 explained nearly 97.2% of the variability.

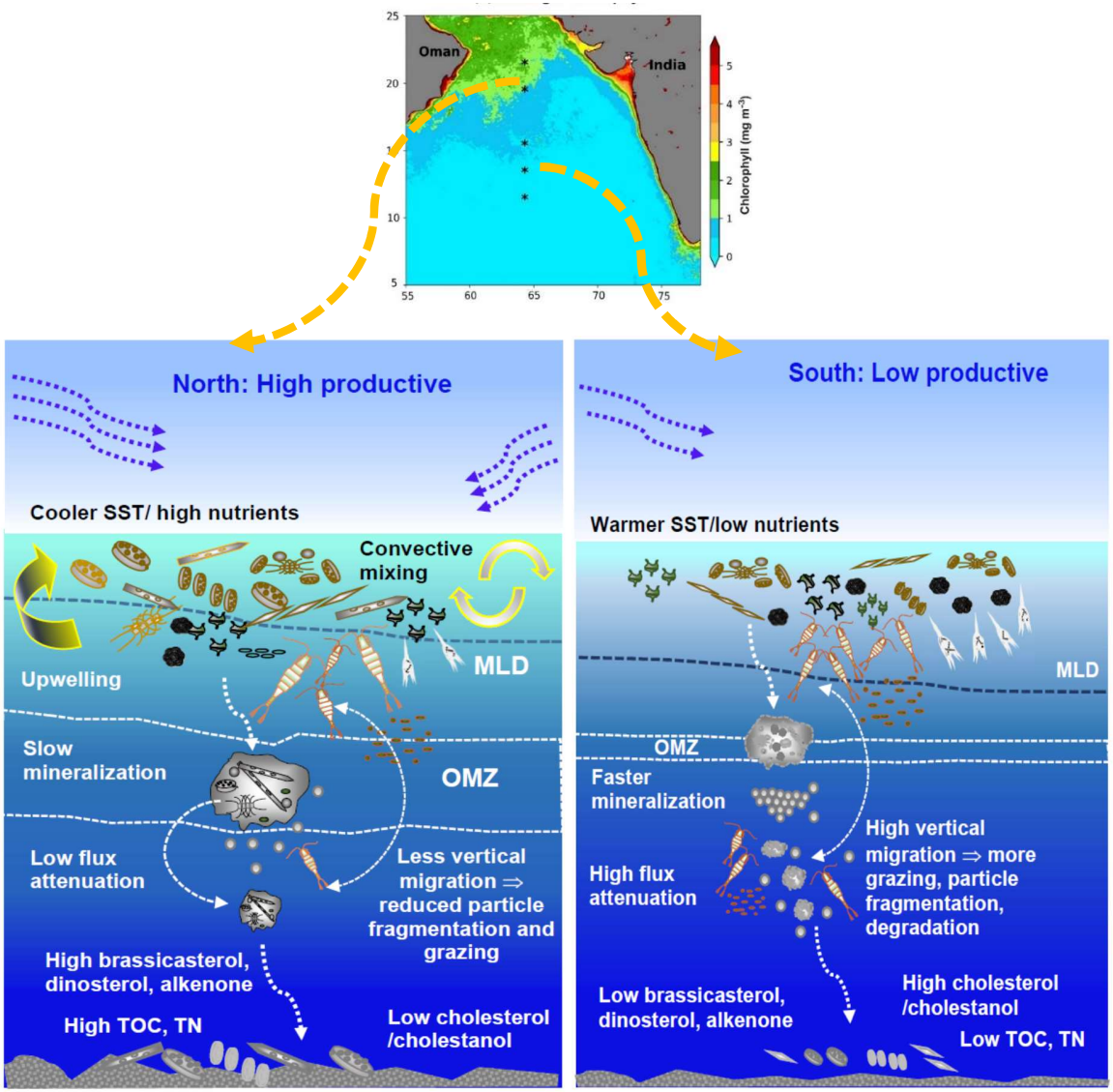

Figure 5. The schematic shows the spatial variability in particle flux along the 64° E transect in the central Arabian Sea.

1178 **Table 1.** Sedimentary characteristics, diatom frustules, and sterol concentrations in the surface sediments from the central Arabian Sea
1179 (n =2±SD). The values represent the average from 0.5 and 1 cm core slices.

Latitude (°N)	21°	19°	15°	13°	11°	Average ±SD
TIC %	3.25±0.15	5.50±0.09	6.70±0.24	7.60±0.13	6.51±0.06	5.91±1.66
TOC %	1.04±0.01	0.91±0.03	0.96±0.03	0.78±0.06	0.79±0.07	0.90±0.11
TN %	0.11±0.001	0.08±0.005	0.07±0.002	0.06±0.003	0.07±0.009	0.08±0.02
TOC:TN	9.5±0.18	10.9±0.28	14±0.08	13.9±1.83	12.1±2.69	12.1±1.9
Alkenone based SST (°C)	27.6±0.05	27.7±0.33	27.5±0.42	27.9±0.36	28.1±0.20	27.8±0.2
Diatom frustule (No.×10^4 valves g^{-1})	5.33±0.83	6.36±0.20	4.69±0.94	3.75±1.43	2.78±0.73	4.58±1.39
Radiolarian (No.×10^4 individuals g^{-1})	1.07±0.36	1.14±0.20	1.57±0.38	2.13±0.39	1.83±0.55	1.54±0.45
Brassicasterol (ng g^{-1})	128.0±52.6	68.6±43.0	58.2±43.5	46.4±24.4	42.0±33.9	68.62±34.77
Dinosterol (ng g^{-1})	171.1±84.4	114.2±51.4	89.8±66.2	61.0±36.7	57.7±38.8	98.76±46.53
Dinostanol (ng g^{-1})	79.0±39.4	48.0±31.5	34.7±35.2	28.3±27.8	29.8±28.0	43.95±21.05
C_{37} alkenone (ng g^{-1})	52.2±6.3	36.0±7.4	39.0±8.0	36.9±19.1	33.3±19.3	39.47±7.39
Cholesterol (ng g^{-1})	113.2±24.4	84.4±23.3	94.1±36.8	132.3±29.5	87.3±42.9	102.27±20.21
Cholestanol (ng g^{-1})	104.4±26.9	93.7±24.6	143.5±115.1	98.6±65.3	141.6±116.5	116.37±24.22
Dinosterol: Brassicasterol	1.31	1.78	1.55	1.28	1.49	1.5±0.2
Brassicasterol: Alkenone	2.41	1.82	1.41	1.25	1.16	1.6±0.5

1180

1181 **Table 2.** Average values of various parameters (n =2, ±SD) from the northern (21, 19, and 15° N) and southern stations (13 and 11° N)
1182 of the central Arabian Sea. The values shown in **bold** "*p*" represent the level of significance (single-factor ANOVA at 95% confidence
1183 level) between the northern and the southern stations.

1184

Parameter	North	South	*p*-value
Total Inorganic Carbon (TIC %)	5.15±1.57	7.06±0.63	**0.05**
Total Organic Carbon (TOC %)	0.97±0.06	0.78±0.05	**0.0009**
Total Nitrogen (TN %)	0.087±0.018	0.061±0.008	**0.03**
Alkenone derived SST (°C)	27.6±0.25	28.0±0.26	**0.043**
Brassicasterol (µg g^{-1} TOC)	8.64±4.75	5.81±3.48	0.3
Dinosterol (µg g^{-1} TOC)	12.81±6.30	7.80±4.47	0.2
Dinostanol (µg g^{-1} TOC)	5.50±3.35	3.87±3.17	0.46
C_{37} alkenone (µg g^{-1} TOC)	4.34±0.81	4.60±2.33	0.8
Cholesterol (µg g^{-1} TOC)	9.99±2.50	14.26±5.83	0.14
Cholestanol (µg g^{-1} TOC)	11.80±6.33	15.85±11.39	0.49
Dinosterol: Brassicasterol	1.55±0.27	1.39±0.21	0.34
Brassicasterol: Alkenone	1.88±0.76	1.21±0.21	0.13
Diatom frustules (No.×10^4 valves g^{-1})	5.46±0.95	3.26±1.08	**0.009**
Radiolarian (No.×10^4 individuals g^{-1})	1.26±0.35	1.98±0.43	**0.019**

1185